

Distinct chemical resistance-inducing stimuli induce common transcriptional, metabolic and nematode community signatures in rice root and rhizosphere

Willem Desmedt^{1,2,3}, Enoch Narh Kudjordjie⁴, Satish Namdeo Chavan^{1,5}, Sandrien Desmet^{2,3,6}, Mogens Nicolaisen⁴, Bartel Vanholme^{2,3}, Mette Vestergård⁴, Tina Kyndt¹

¹ Research Group Epigenetics and Defence, Department of Biotechnology, Ghent University, 9000 Ghent, Belgium;

² Department of Plant Biotechnology and Bioinformatics, Ghent University, 9052 Ghent, Belgium

³ VIB Center for Plant Systems Biology, 9052 Ghent, Belgium

⁴ Department of Agroecology, Faculty of Technical Sciences, Aarhus University, 4200 Slagelse, Denmark

⁵ ICAR-Indian Institute of Rice Research, Rajendranagar, 500030 Hyderabad, India

⁶ VIB Metabolomics Core Ghent, 9052 Ghent, Belgium

Author e-mail addresses: WD - willem.desmedt@ugent.be; ENK - enochnarh@agro.au.dk; SNC - satish.namdeochavan@ugent.be; SD - sandrien.desmet@psb.ugent.be; MN - mn@agro.au.dk; BV - bartel.vanholme@ugent.be; MV - mvestergard@agro.au.dk; TK - tina.kyndt@ugent.be

Corresponding author: Tina Kyndt (tina.kyndt@ugent.be)

Highlight

A comparison of chemical resistance-inducing stimuli in rice reveals conserved systemic transcriptional and metabolic responses that affect rhizosphere nematode communities in ways that might contribute to the induced resistance phenotype.

Abstract

Induced resistance (IR), a phenotypic state induced by an exogenous stimulus and characterized by enhanced resistance to future (a)biotic challenge, is an important component of plant immunity. Numerous IR-inducing stimuli have been described in various plant species, but relatively little is known about 'core' systemic responses shared by these distinct IR stimuli and the effects of IR on plant-associated microbiota. In this study, we foliarly applied four distinct IR stimuli (β -aminobutyric acid, acibenzolar-S-methyl, dehydroascorbic acid and piperonylic acid) capable of inducing systemic IR in rice (*Oryza sativa*) against the root-knot nematode *Meloidogyne graminicola* and evaluated their effect on the root transcriptome, exudome and root-associated nematode communities. Our results reveal shared transcriptional responses –notably induction of jasmonic acid and phenylpropanoid metabolism – and shared alterations to the exudome that include increased amino acid, benzoate and fatty acid exudation. In rice plants grown in soil from a rice field, IR stimuli significantly affected the composition of rhizosphere nematode communities three days after treatment, but by 14 days after treatment these changes had largely reverted. Notably, IR stimuli did not reduce nematode diversity, which suggests that IR might offer a sustainable option for managing plant-parasitic nematodes.

Keywords: acibenzolar-S-methyl, β -aminobutyric acid, dehydroascorbic acid, induced resistance, *Meloidogyne*, metabarcoding, metabolomics, piperonylic acid, priming, root exudates

Accepted Manuscript

Abbreviations

BABA	β -aminobutyric acid
BTH	benzothiadiazole (acibenzolar-S-methyl)
DHA	dehydroascorbic acid
FDR	false discovery rate
GC-MS	gas chromatography-mass spectrometry
GO	gene ontology
IR	induced resistance
JA	jasmonic acid
LFC	log-fold change
NMDS	Non-metric multi-dimensional scaling
NW	NemaWater
PPP	phenylpropanoid pathway
ROS	reactive oxygen species
SA	salicylic acid
SAP	sand-absorbent polymer
PA	piperonylic acid
PCA	principal component analysis
PR	pathogenesis-related
WCGNA	weighted gene co-expression network analysis

Introduction

Induced resistance (IR) refers to a phenotypic state in plants that is induced by an external stimulus and which is characterized by enhanced resistance to future (a)biotic stressors (de Kesel *et al.*, 2021). IR may be induced by diverse stimuli, including beneficial microbes, herbivory, abiotic stress and certain chemicals (Mauch-Mani *et al.*, 2017). While most studies on IR focused on a handful of model pathosystems, notably foliar pathogens of *Arabidopsis thaliana* (Cohen *et al.*, 2016; Mauch-Mani *et al.*, 2017), IR occurs in both wild and cultivated plant species, and in a wide range of plant tissues and organs (Cohen *et al.*, 2016; Mauch-Mani *et al.*, 2017; de Kesel *et al.*, 2021).

In rice, a crop species often used as a model for monocot plants, the existence of IR against several important rice pests and pathogens has been confirmed. The most economically significant IR stimuli in rice are salicylic acid (SA) analogs such as probenazole, which are used to control rice blast (caused by the fungal pathogen *Magnaporthe oryzae*) and leaf blight (caused by the bacterial pathogen *Xanthomonas oryzae*) in commercial rice cultivation (Iwata, 2001). Various other IR stimuli, including acibenzolar-S-methyl (also known as benzothiadiazole; De Vleeschauwer *et al.*, 2008) and nonpathogenic IR-inducing *Pseudomonas* strains (De Vleeschauwer *et al.*, 2008), also show potential against foliar rice pests and diseases in growth chamber conditions.

By contrast, only a limited body of literature has been published on IR stimuli against root pests or pathogens of rice. Most of this literature has focused on the interaction between rice and the root-knot nematode *Meloidogyne graminicola*, one of the most devastating pests of rice (Mantelin *et al.*, 2017). Examples of chemical IR stimuli effective in this pathosystem include β -aminobutyric acid (BABA; Ji *et al.*, 2015), acibenzolar-S-methyl/benzothiadiazole (BTH; Nahar *et al.*, 2011), piperonylic acid (PA; Desmedt *et al.*, 2021a, 2022), dehydroascorbic acid (DHA; Singh *et al.*, 2020), thiamine (Huang *et al.*, 2016) and diproline (De Kesel *et al.*, 2020). Interestingly, most of these stimuli induce resistance to *M. graminicola* when applied to rice shoots. Conversely, several of the IR stimuli mentioned above induce IR against shoot pathogens when applied as a soil drench (Iwata, 2001; De Vleeschauwer *et al.*, 2008). IR in rice is thus a systemic process, as is the case in dicot plants such as *A. thaliana*, tobacco and tomato (Vlot *et al.*, 2021). While the systemic nature of IR in rice and other monocots remains poorly understood, in *A. thaliana* IR spreads systemically through the action of various signaling molecules, including glycerol-3-phosphate, methyl salicylate, pipercolic acid and its catabolite N-hydroxypipercolic acid, and azelaic acid (Vlot *et al.*, 2021). At the phytohormone level, IR in dicots may depend on either the SA, jasmonic acid/ethylene (JA/ET) or abscisic acid (ABA) pathways, or may be hormone-independent. JA/ET signaling has traditionally been associated with *induced systemic resistance* (ISR), a form of IR induced by beneficial root-associated microbes (van Loon *et al.*, 1998; Van Wees *et al.*, 2008; Vlot *et al.*, 2021). By contrast, SA signaling has, together with pipercolic acid signaling, been described as the main driver of *systemic acquired resistance*, a form of IR induced by exposure to necrotizing leaf pathogens (de Kesel *et al.*, 2021; Vlot *et al.*, 2021). However, the many exceptions to this dichotomy have led to the view that the umbrella term IR is preferable (de Kesel *et al.*, 2021).

IR has a *direct* and a *primed* component. The former consists of responses triggered upon perception of the IR stimulus, whereas the latter describes responses that only occur when the treated plant is subsequently exposed to an (a)biotic challenge (de Kesel *et al.*, 2021). Both phases of the IR response involve extensive transcriptional, epigenetic and metabolic alterations (Mauch-Mani *et al.*, 2017). At

the metabolic level, the direct response involves, amongst others, alterations to primary metabolism (notably the abundance of free amino acids, sugars and tricarboxylic acid cycle intermediates) and induction of phenylpropanoid pathway (PPP) metabolism (Tugizimana *et al.*, 2018). Primed metabolic responses are more diverse and may include enhanced accumulation of phytoalexins, SA, JA, or phenylpropanoids (Tugizimana *et al.*, 2018).

While several studies have examined the metabolome of plants treated with chemical IR stimuli (Tugizimana *et al.*, 2018; Luna *et al.*, 2020; Desmedt *et al.*, 2021a), their effect on the exudome – the diverse array of primary and secondary metabolites exuded by plant roots – remains unexplored. The exudome plays a key role in shaping plant-pathogen interactions, both directly by affecting the behavior and survival of pathogens and indirectly by promoting recruitment of beneficial microorganisms (Baetz and Martinoia, 2014; van Dam and Bouwmeester, 2016; Sikder and Vestergård, 2020; Rizaludin *et al.*, 2021).

We hypothesized that systemic IR induction in rice by chemically distinct IR stimuli effective against *M. graminicola* would induce common perturbations in the rice root transcriptome and exudome, and that this would in turn affect rice-associated nematode communities. To investigate this hypothesis, we analyzed the root transcriptome (using mRNA-sequencing) and exudome (using GC-MS) upon treatment with IR stimuli, and used metabarcoding to study the structure of rice-associated nematode communities in rice plants grown in soil from a rice field and treated with IR stimuli. To the best of our knowledge, our study is the first to identify common responses to IR stimuli in rice and to provide insights into the effect of IR stimuli on plant-nematode interactions in the rice rhizosphere.

Materials and methods

Nematode infection experiment

Rice (*Oryza sativa* L. subsp. *japonica* 'Kitaake') seeds were germinated on moist tissue paper in sealed petri dishes in the dark for five days at 28°C before being transplanted to individual PVC tubes (height: 15 cm, diameter: 3 cm) filled with a mixture of sand and absorbent polymer (SAP) (Reversat *et al.*, 1999). The tubes were placed in a growth chamber (28°C, 12:12 light:dark), and seedlings were watered three times per week with 10 ml half-strength Hoagland solution as described in (Nahar *et al.*, 2011). Seedlings were foliarly treated by spraying seedlings until run-off with the tested compound (*R,S*- β -aminobutyric acid (BABA), piperonylic acid (PA), benzothiadiazole (BTH) or dehydroascorbic acid (DHA)) dissolved in distilled water amended with 0.1 vol% Tween 20 surfactant. BABA, PA and DHA were purchased from Sigma-Aldrich, whereas BTH was kindly provided by Syngenta as the formulated product ActiGard 50WG.

The four IR stimuli were applied at concentrations and time points previously reported to be effective at inducing resistance to *Meloidogyne graminicola*: BABA (3.5 mM, 14 days post transplantation (dpt); Ji *et al.*, 2015), BTH (250 μ M, 14 dpt; Nahar *et al.*, 2011), DHA (20 mM, 14 dpt; Chavan *et al.*, 2022) and PA (300 μ M, 8 and 14 dpt; Desmedt *et al.*, 2021). Mock-treated control plants were sprayed with distilled water containing 0.1 vol% Tween 20 at the same time points.

M. graminicola was cultured on *Echinochloa crus-galli* (24°C, 16:8 light:dark). Second-stage juveniles (J2s) were extracted using a modified Baermann funnel and the resulting nematode suspension was

diluted with sterile tap water to a density of 125 J2s per ml. Two-week old rice seedlings were inoculated by pipetting 2 ml of the *M. graminicola* suspension next to the root system with a micropipette. Plants were harvested 14 days post inoculation, and shoot and root length were measured. Root systems were stained with acid fuchsin (Byrd *et al.*, 1983) and destained in acidified glycerol (glycerol + 1 ml l⁻¹ 37% HCl) for one week before counting the number of galls per root system using a stereo microscope. Gall numbers between treatments were compared using a Kruskal-Wallis test ($p < 0.05$) followed by a Conover-Iman post-hoc test, both performed using the *PMCMRplus* package v. 1.9.3 in R v. 4.1.2.

mRNA sequencing

Rice seedlings (*O. sativa* 'Kitaake') were grown and treated in the same way as for infection experiments. Seedlings were treated when they were 14 days old, and 24 h later root systems were gently washed, flash-frozen in liquid nitrogen and ground in a nitrogen-cooled pestle and mortar. Roots from five seedlings were pooled to form one sample, and three pooled samples were created per treatment. Plants treated with BTH, BABA or PA, and their corresponding control plants, were grown by the author for this study; mRNA-seq on DHA-treated plants and their control plants was performed earlier (Chavan *et al.*, 2022). The same growth chamber, light and temperature settings on a batch of Kitaake seeds were used for both experiments.

RNA was extracted from approximately 100 mg of ground root tissue using a Qiagen RNeasy Plant Mini Kit according to the manufacturer's instructions, with one modification: after addition of buffer RLT, samples were sonicated three times for 20 seconds each time at 40 kHz in an ice bath (Branson Bransonic 1800 CPX). RNA purity and quantity were assessed using a NanoDrop spectrophotometer (ThermoFisher Scientific), and RNA integrity was verified using an Agilent BioAnalyzer 2100. Library preparation and sequencing, as well as trimming and mapping the resulting reads, were performed as described in (Ghaemi *et al.*, 2020).

To identify differentially expressed (DE) genes between plants treated with IR stimuli and their mock-treated controls, *DeSeq2* v. 1.32.0 (Love *et al.*, 2014) was used (threshold: FDR-adjusted $p < 0.10$ and $|\log_2\text{-fold change}| > 0.5$). Genes that were differentially expressed after treatment with at least three out of the four tested IR stimuli were retained and annotated by matching against the RAPDB database, with manual curation. Gene ontology (GO) enrichment analysis using PLAZA 4.5 (Van Bel *et al.*, 2018), g:Profiler (Raudvere *et al.*, 2019) and MapMan (Thimm *et al.*, 2004) was then performed on this list.

Gene co-expression network analysis was performed in R v. 4.1.2. Since this requires normalized count data rather than on fold change data, and because a significant batch effect was apparent in our data that persisted even after using the *ComBat_seq* function (Zhang *et al.*, 2020) in the *sva* package v. 3.40.0 (Zhang *et al.*, 2020), DHA was excluded from this network analysis. The *geneFilter* package v. 1.74.1 was used to filter out genes with an interquartile range below 0.5, after which gene co-expression was analyzed using weighted gene correlation network analysis was performed using *WGCNA* v. 1.70-3 (Langfelder and Horvath, 2008). The *pickSoftThreshold* function was used to identify the optimal power for the network, and then a signed network was inferred using the *blockwiseModules* function with robust biweight midcorrelation ('bicor') and a minimal block size of 90. The Pearson correlation coefficient to each treatment was calculated for each module using the *cor* and *corPvalueStudent* functions in the *WGCNA* package. The putative biological role of each

module was inferred using the g:Profiler GO analysis tool, and the overlap between each module and the 'core' gene set identified using DE analysis was quantified.

Exudate profiling

Rice seedlings (*O. sativa* 'Kitaake') were grown as described above until twelve days post transplantation, so that exudates were collected at the same stage as sampling for mRNA sequencing. Seedlings were carefully removed from SAP, washed and placed in glass test tubes containing 20 ml sterile half-strength Hoagland solution (five seedlings per tube, five tubes per treatment). The tubes were plugged with cotton wool and returned to the same growth chamber conditions. After six hours, plants were foliarly treated with BABA (3.5 mM), BTH (250 μ M) or PA (300 μ M). Twenty-four hours after treatment with resistance inducers, 12 ml NemaWater, a mixture of *M. graminicola*-derived pathogen associated molecular patterns (PAMPs) used to imitate nematode infection, was added at a concentration of 150 nematode equivalents per ml to half of all tubes. The other half was mock-treated by adding 12 ml of filter-sterilized tap water. NemaWater was prepared as described in (De Kesel *et al.*, 2020). Briefly, a suspension containing 150 freshly extracted *M. graminicola* J2s per ml was incubated overnight at room temperature on an orbital shaker. Nematodes were then removed by centrifugation, and the supernatant was collected and filter-sterilized (0.22 μ m pore diameter PES syringe filter, NovoLab) to yield NemaWater at a concentration of 150 'nematode equivalents per ml'. Exudates were collected four days after transfer to hydroponic solution using Bond Elut Plexa C18 LRC cartridges (Agilent, 100 mg bed mass). Columns were conditioned by washing with 0.75 ml methanol and then with 0.75 ml distilled water, after which exudates were filtered through the conditioned bed and washed with 0.75 ml 10% methanol before being eluted with 1.0 ml methanol. The eluent was dried *in vacuo* and kept at -80°C until analysis.

Samples were then trimethylsilylated using 100 μ l derivatization mixture (*N*-methyl-*N*-(trimethylsilyl)trifluoroacetamide:pyridine in a 5:1 ratio). GC-MS analyses were performed on an Agilent 7250 QTOF-MS with an Agilent 7890B GC system. One microliter of derivatized sample was injected in splitless mode with the injector port set to 280°C. Separation was achieved with a VF-5ms column (30 m \times 0.25 mm, 0.25 μ m; Varian CP9013; Agilent) with helium carrier gas at a constant flow rate of 1.2 ml/min. The oven was held at 80°C for 1 min, ramped to 320°C at a rate of 5°C/min and then held at 320°C for 10 min before being cooled to 80°C at 50°C/min at the end of the run. The injector, MS transfer line, MS ion source and quadrupole were held at 280°C, 280°C, 230°C and 150°C respectively. The MS detector was operated in EI mode at 70 eV. Full EI-MS spectra were recorded by scanning the *m/z* range of 50 to 800 with a solvent delay of 7.8 min. Feature extraction and chromatographic alignment was performed using Agilent MassHunter Profinder v. 10.0; only peaks with a peak height over 300 counts and which were detected in at least two samples per treatment group were retained. The resulting features were matched against the NIST/EPA/NIH EI-MS 2020 (NIST20) library to allow tentative identification based on MS spectra.

As an exploratory data analysis, principal component analysis (PCA) score plots and heatmaps were generated in MetaboAnalyst 5.0 (Pang *et al.*, 2021) using log-transformed, Pareto-scaled data. Next, peak areas of features were compared between mock-treated samples and samples treated with BABA-, BTH-, PA- or NemaWater using pairwise heteroskedastic t-tests with false discovery rate (FDR) adjustment. Features which were significantly differentially abundant after treatment with at least three out of four stimuli were retained. The same procedure was also used to identify features

whose abundance was *primed*, i.e. which were more abundant in exudates from plants treated with PA, BABA or BTH and then elicited with NemaWater versus those that were mock-treated prior to elicitation by NemaWater.

Nematode community analysis

Soil from a rice field with a long history of rice cultivation and a diagnosed *M. graminicola* infestation, located in the commune of Garlasco (Pavia province, Lombardy, Italy), was collected on August 26th, 2021. A number of rice plants in the middle of the field were uprooted and approximately 30 kg of soil was collected from this spot and kept in sealed plastic bags until use. The soil was a loam soil, with approximately 50% sand, 40% loam and 10% clay. Rice plants growing in this part of the field showed a galling index of 7-8 on the Bridge scale, indicating a relatively severe *Meloidogyne* infestation. The soil had an average pH (\pm SD) of 6.11 ± 0.03 , determined by suspending four 15 g soil samples in 30 ml of distilled water each and measuring soil pH using a pH meter (Metrohm 827 Lab) after 30 minutes of incubation on an orbital shaker.

Upon arrival in the lab (September 6th, 2021), residual plant material, rocks and clumps were removed and the remaining soil was mixed thoroughly. To assess the soil's baseline nematode density, six 30 ml samples were taken at random from the soil, from which nematodes were extracted using an Oostenbrink dish kept at room temperature for four days. The resulting suspension was concentrated by centrifugation and examined using a binocular microscope. The total number of nematodes and of the number of plant-parasitic nematodes per liter of soil was then calculated. An average (\pm SD) of 4440 ± 650 nematodes per liter of soil were recovered, of which 433 ± 120 were plant-parasitic.

Rice seeds (*O. sativa* 'Kitaake') were germinated as described previously and transplanted to individual plastic pots filled with 250 ml of field soil each. Pots were placed in a greenhouse compartment at AU Flakkebjerg (Slagelse, Denmark) kept at 26°C throughout the experiment, with 12 h of artificial light per day. For the first 24 h after transplantation, seedlings were covered with a transparent plastic sheet. Pots were watered with 70 ml of distilled water upon transplantation, and daily with 15 ml of distilled water from that point onwards. Seedlings were fertilized twice, at one and 14 days post transplantation, with 20 ml of a fertilizer solution containing 2 g/l ferrous sulfate heptahydrate and 1 g/l ammonium sulfate. To compensate for the low number of plant-parasitic nematodes observed in the soil samples, pots were inoculated by adding 120 *M. graminicola* J2s to the corner of each pot, eight days post transplantation. Seven and 14 days after transplantation, seedlings were sprayed with either PA (300 μ M), BABA (3.5 mM) or BTH (250 μ M) until run-off; all spraying solutions were amended with 0.1 vol% Tween 20 surfactant. Control plants were sprayed with a solution containing only 0.1 vol% Tween 20 at the same time point.

Seventeen days after transplantation, five seedlings from each treatment were carefully uprooted. As described in (Sikder *et al.*, 2021a), root systems were gently shaken until non-adherent soil was removed, after which the adherent (rhizosphere) soil was gently scraped off and flash-frozen in liquid nitrogen. Root systems were then thoroughly washed clean with distilled water and frozen separately. The remaining five seedlings from each group were harvested in an identical manner 14 days after treatment (dat), i.e. four weeks after transplantation.

Root and rhizosphere samples were freeze-dried for 48 h, and then ground for 3 x 1 min at 1500 strokes per minute in a GenoGrinder (Ramcon). DNA was extracted from the freeze-dried soil samples using a Qiagen PowerLyzer Soil kit, and from root samples using a Qiagen DNEasy Plant Pro kit. After checking each sample's DNA concentration using a Qubit fluorometer (Thermo-Fisher Scientific), the V6-V8 region of the nematode 18S rRNA gene was amplified using the Nemf/18Sr2b PCR primer sets and conditions described in (Sikder *et al.*, 2020). PCR products were diluted (1:5) and pooled, and a second PCR was then performed for dual indexing, again using the primers and conditions described in (Sikder *et al.*, 2020). All amplicons were visualized by gel electrophoresis, pooled, precipitated, and redissolved in TE buffer (pH 8.0). Pooled DNA was run on a 1.5% agarose gel, from which amplicons were excised and purified using a Qiagen QIAquick Gel Extraction kit according to the manufacturer's instructions. Finally, the resulting library's DNA concentration and purity were verified using a Qubit fluorometer and gel electrophoresis before sending the library for sequencing on an Illumina MiSeq sequencer with PE300 (Eurofins Genomics).

Data were processed as described in (Sikder *et al.*, 2021a). Briefly, reads were demultiplexed, merged (minimal overlap 10 bp) and filtered using *vsearch* v. 2.6 (Rognes *et al.*, 2016), implemented in *qiime2* (Bolyen *et al.*, 2019). Reads shorter than 250 bp or with Phred score < 30 were removed, as were internal barcodes, forward and reverse primers, duplicates and chimeras. Sequences were clustered into operational taxonomic units (OTUs) using *vsearch* v. 2.6 with a similarity threshold of 99%. OTUs were then blasted against the NCBI database for identification (threshold: 100% similarity for species, 99% for genus; BLAST method: megablast, default parameters). Further analyses were performed in R v. 4.1.2. Bray-Curtis dissimilarity matrices were visualized using non-metric multi-dimensional scaling (NMDS) as implemented in the *vegan* package v. 2.5-7 (Oksanen *et al.*, 2009) (*metaNMDS* function, $k = 3$), and used for permutational analysis of variance (PERMANOVA) through the *adonis* function. OTUs were then grouped per genus, and the resulting table was transformed to relative abundances. Simpson's diversity index was used to estimate alpha diversity using the *diversity* function in *vegan*, and the abundance of each genus was compared using the Kruskal-Wallis test followed by a post-hoc Conover-Iman test (using *PMCMRplus* v. 1.9.3). Differential abundance was also assessed directly on read count data (without prior transformation to relative abundances) using *DeSeq2* v. 1.32.0 (Love *et al.*, 2014).

Results

Four chemically distinct IR stimuli induce systemic resistance against M. graminicola

In agreement with previously published results (Nahar *et al.*, 2011; Ji *et al.*, 2015; Singh *et al.*, 2020; Desmedt *et al.*, 2021a), pre-treatment with 3.5 mM β -aminobutyric acid (BABA), 300 μ M piperonylic acid (PA), 250 μ M benzothiadiazole (BTH) or 20 mM dehydroascorbic acid (DHA) reduces rice susceptibility to the root-knot nematode *M. graminicola* (**Figure 1a**). As previously shown, two applications of PA are required to induce full resistance (Desmedt *et al.*, 2021a, 2022); for this reason, further experiments were performed on plants treated with PA twice. BABA, BTH and PA caused no phytotoxicity and had no effect on plant growth (**Figure 1b-c**). By contrast, DHA application slightly reduced median shoot and root length by the end of the experiment (-4% and -14% compared to the mock-treated control, respectively) and resulted in the formation of brown lesions on treated leaves (**Supplementary Figure S2**)

Common transcriptional signatures of systemic IR in rice roots

To establish whether foliar treatment with different chemical IR stimuli affects the expression of a common core set of genes in rice roots, mRNA sequencing was performed on RNA extracted from rice roots 24 h after foliar treatment with BABA, BTH, DHA or PA. Genes or pathways differentially expressed (DE) in response to treatment by four chemically highly distinct stimuli are likely to be causally involved in systemic IR in rice roots, and would thus be of interest to further investigate the molecular basis of the IR phenotype.

Exploratory principal component analysis (PCA; **Figure 2a**) shows that the transcriptomes of rice roots treated with IR stimuli are all clearly distinct from mock-treated samples, indicating significant transcriptional reprogramming in rice roots after foliar application of IR stimuli. The confidence ellipses of the IR stimuli overlap partially, which suggests that the different stimuli induce both shared and distinct transcriptional effects.

Genes whose expression differs significantly between BABA, BTH, PA or DHA-treated plants and their mock-treated controls were identified using DeSeq2 (**Figure 2b**). The number of such genes varied widely between the four treatments, but was biased towards upregulation: 301 DE genes for BABA (255 upregulated, 46 downregulated), 788 DE genes for BTH (596 upregulated, 192 downregulated), 2365 DE genes for DHA (1519 upregulated, 846 downregulated) and 406 DE genes for PA (329 upregulated, 77 downregulated).

A total of 76 genes were significantly DE after treatment with all four IR stimuli (**Figure 2b**), of which only two were downregulated and 74 were upregulated. These genes, and their (putative) annotations, are listed in **Table 1**. A further 88 genes were up- or downregulated by three out of four stimuli; these genes are listed in **Supplementary Table S1**.

The common 'core' genes listed in **Table 1 and Supplementary Table S1** are notably enriched for: (1) genes related to phenylpropanoid pathway metabolism, (2) genes encoding pathogenesis-related (PR) proteins, (3) genes related to jasmonic acid metabolism and (4) genes encoding transcription factors. This is supported by three different gene ontology (GO) enrichment analysis tools: g:Profiler (Raudvere *et al.*, 2019), PLAZA (Van Bel *et al.*, 2018) and MapMan (Thimm *et al.*, 2004) (**Supplementary Table S2**). Phenylpropanoid pathway (PPP) metabolism enrichment is identified by all three tools, PR genes (under the generic GO terms 'response to wounding', 'response to external biotic stimulus' and 'response to fungus') are identified by g:Profiler and PLAZA, while JA and transcription factors are identified by one tool each (g:Profiler and MapMan respectively).

Gene co-expression network analysis of the rice root IR transcriptome

In addition to DE analysis, the effect of IR on the root transcriptome was also analyzed using weighted gene co-expression network analysis (WCGNA) to identify groups of genes (modules) with a shared expression profile across samples and treatments. WCGNA analysis identified 28 such modules, ranging in size from 102 to 1501 genes. Of these 28 modules, five were significantly negatively correlated with mock-treated samples and predominantly positively correlated with IR-treated groups, and a further five were significantly positively correlated with mock-treated samples and predominantly negatively correlated to IR-treated groups (**Supplementary Table S3**).

Five of those eight modules (named M3, M6, M17, M14, and M12 in **Supplementary Table S3**) were enriched in the 'core' genes identified using DE analysis. In these five modules, core genes represented between 2.3 and 7.0% of all module members, whereas in the other modules they were either entirely absent (15 modules) or represented less than 1% of module members (8 modules). As these five modules showed both an interesting WCGNA correlation pattern and overlapped with the outcome of our DE analysis, they were analyzed further.

GO analysis (**Supplementary Table S4**) showed that M3 was enriched in both JA and PPP-related gene ontology terms, suggesting that these two pathways are co-regulated during the IR response. M14 appears to be involved in immune signaling: it is exclusively enriched in GO terms related to signaling, and is also enriched in the KEGG pathway 'plant-pathogen interactions'. M17 is highly enriched in GO terms related to transcription and transcription factor activity, suggesting a role in regulating gene expression after treatment with IR stimuli. M12, which is negatively correlated to the mock treatment, contains numerous GO term related to iron homeostasis, possibly indicating a role for iron homeostasis in IR in rice roots. Finally, M6 is a highly heterogeneous module for which GO analysis identified no clear biological function.

Foliar application of chemical IR stimuli alters rice root exudate composition

GC-MS based metabolomics was used to profile rice root exudates from plants foliarly treated with the IR stimuli BTH, BABA or PA and subsequently challenged with NemaWater. NemaWater is a solution of *M. graminicola*-derived PAMPs that induces similar transcriptional responses in treated plants as actual nematode infection (Mendy *et al.*, 2017) and which – unlike actual nematode infection – can be used in the hydroponic setting required for exudate analysis. Plants were induced with an IR stimulus and treated with NemaWater 24 h later. Exudates were then collected and purified through solid phase extraction three days after application of NemaWater.

Exploratory principal component (PCA) analysis (**Figure 3a**) shows that BABA and PA treatments induce exudate profiles clearly distinct from those seen in mock-treated samples, whereas BTH treatment more subtly affects the exudome. All groups respond to NemaWater exposure similarly, as evidenced by a shift towards the upper-right corner of the PCA scores plot (**Figure 3a**). Mock-treated plants are no longer distinguishable from BABA- or BTH-treated plants after induction with NemaWater, indicating that most of the responses induced by these IR stimuli are also induced by exposure to NemaWater – suggesting that IR induction and PAMP-triggered immunity (PTI) are highly similar processes.

Each of the individual treatments substantially affected the composition of rice root exudates. A total of 993 features ('metabolites') were reliably detected; treatment with BABA, BTH, PA or NemaWater altered the abundance of respectively 217, 105, 343 and 302 of those. Out of the 302 metabolites differentially abundant between mock- and NemaWater-treated samples at least some are likely components of the NemaWater itself rather than exuded metabolites.

To identify putative 'core' IR-related rice root exudates, features which were significantly differentially abundant after treatment with at least three out of four of the individual treatments (BABA, BTH, PA or NemaWater) were sought. A total of 46 features were affected by all four stimuli, and 89 were affected by three (**Figure 3d**). Of those features, 35 could be annotated with a high degree of confidence (NIST match factor ≥ 70 ; **Table 2**), and 40 were tentatively annotated with a low

degree of confidence (NIST match factor 50-70; **Supplementary Table S6**). In general, IR stimuli increase amino acid exudation, and possibly also the exudation of sugars, sugar alcohols, fatty acids and phenylpropanoid pathway derivatives (particularly benzoates).

While all tested IR stimuli had substantial, partially overlapping effects on the exudome, there was less evidence for a common primed response upon subsequent challenge with NemaWater. In plants pre-treated with BABA or PA that were then challenged with NemaWater, 20 and 144 features respectively were differentially abundant relative to mock-treated plants induced with NemaWater. Only one feature was significantly primed by BTH. No common features were primed by all three stimuli, and just 8 were primed by both BABA and PA.

IR stimuli alter rhizosphere nematode communities

Since IR stimuli enhance rice resistance to *M. graminicola* (**Figure 1**) and alter root exudate composition (**Table 2**), we hypothesized that foliar application of these stimuli might affect the structure of rice root-associated nematode communities. To investigate this hypothesis, we grew rice seedlings in soil sampled from a field with a long history of rice cultivation and a diagnosed *M. graminicola* infestation. Seventeen and 28 days after transplantation to soil, i.e. 3 and 14 days after foliar treatment with BABA, BTH or PA, seedlings were uprooted and their roots and the adherent rhizosphere soil were collected separately. Metabarcoding with primers targeting the V6-V8 region of the nematode 18S rRNA gene followed by sequencing of the resulting amplicons was used to characterize nematode communities in the rice root and rhizosphere compartments. After removing low-quality reads and reads that could not be assigned to the phylum Nematoda, 546 641 reads assigned to 54 different operational taxonomic units (OTUs) were retained. Of these OTUs, 33 of those could be identified to genus level.

Exploratory analysis using non-metric multidimensional scaling (**Figure 4**) reveals that IR stimuli profoundly affect rhizosphere nematode communities 3 days after treatment (dat) (**Figure 4a**), but that by 14 days the rhizospheres of BTH- or PA-treated plants no longer differ substantially from those of mock-treated plants (**Figure 4c**). By contrast, the effect of BABA treatment appears more persistent, as the rhizosphere nematode community remains highly distinctive 14 dat. Nematode communities inside plant roots show much more subtle alterations at both 3 and 14 dat (**Figure 4b** and **d**). These observations are supported by permutational analysis of variance (PERMANOVA; **Table 3**), which finds significant differences in rhizosphere composition 3 dat for all tested IR stimuli, but only for BABA at 14 dat. Communities inside the root are also affected by IR treatment at 3 dat, but not at 14 dat. There are no differences in alpha diversity (measured using Simpson's diversity index) at either time point in root or rhizosphere samples (**Supplementary Figure S1**).

Our analysis showed that 3 days after the final treatment with IR stimuli, rhizosphere nematode communities of BABA-, BTH- or PA-treated plants were all altered in similar ways (**Figure 5a**): the percentage of reads attributable to the genus *Acrobeloides* is reduced (24%, 23% and 30% respectively, versus 54% in mock-treated plants; $p < 0.01$), while the proportion of reads from minor genera is increased (47%, 41% and 45% respectively, versus 15% in mock-treated plants; $p < 0.01$). Rhizosphere communities of IR-treated plants are also highly enriched in the predatory nematode genus *Mononchus* (4.4%, 7.9% and 4.7% in BABA-, BTH- and PA-treated samples respectively, versus 0.7% in mock-treated plants; $p = 0.04$).

Fourteen dat (**Figure 5c**), rhizosphere communities of plants treated with IR stimuli were no longer significantly enriched in minor genera. The reduced relative abundance of *Acrobelloides* had also largely disappeared in BTH- and PA-treated plants (32% and 37% respectively, versus 39% in mock-treated plants; $p = 0.34$ and $p = 0.34$), but persisted in BABA-treated plants, where *Acrobelloides* accounted for just 25% of reads ($p = 0.04$). BABA-treated plants were instead significantly enriched in the genus *Prismatolaimus*, which accounted for 21% of reads in BABA-treated samples versus just 9% in mock-treated plants ($p = 0.02$), 4% in BTH-treated plants ($p = 0.20$) and 6% in PA-treated plants ($p = 0.22$). The enrichment of *Mononchus* in rhizospheres of plants treated with IR stimuli remained visible after 14 days: this genus accounted for just 0.3% of reads in mock-treated plants, versus 2.2% in BABA-treated samples ($p = 0.04$), 4.1% in BTH-treated samples ($p = 0.02$) and 3.0% in PA-treated samples ($p < 0.01$). Another minor genus that showed significant enrichment was *Thonus*, a poorly characterized genus of mostly omnivorous, occasionally predatory, nematodes (Yeates *et al.*, 1993). *Thonus* accounted for 0.0% of reads in the mock-treated samples, 0.7% of reads in BABA-treated samples ($p < 0.01$), 2.4% in BTH-treated samples ($p < 0.01$) and 0.6% in PA-treated samples ($p = 0.01$). Taken together, these results indicate that most changes in rhizosphere nematode community structure induced by IR stimuli seen at 3 dat are transient and have mostly vanished by 14 dat – with the notable exception of persistent enrichment of the genus *Mononchus*.

As already indicated by the NMDS plots, and in marked contrast to the substantial shifts in rhizosphere nematode communities, root nematode community structure in plants treated with IR stimuli differed little from those of mock-treated plants. Three dat (**Figure 5b**), all root samples were dominated by *Meloidogyne*, which accounted for 90% of reads in mock-treated plants, 95% in BABA-treated plants, 96% in BTH-treated plants and 82% in PA-treated plants ($p = 0.06$). None of the minor genera showed statistically significant differences between treatments. By 14 dat (**Figure 5d**), the proportion of *Meloidogyne* had fallen sharply, to 34% in mock-treated plants, 34% in BABA-treated plants, 39% in BTH-treated plants and 24% in PA-treated plants. However, there was again no statistically significant difference between treatments for either *Meloidogyne* ($p = 0.76$) or any other genus.

Differential abundance analysis using DeSeq2 broadly confirms these observations (**Table 4**). This method also identifies a depletion of *Acrobelloides* in the rhizosphere of plants treated with IR stimuli at 3 dat, and enrichment of minor genera and *Mononchus*. This depletion of *Acrobelloides* persists at 14 dat in BABA-treated plants, and to a lesser extent in PA-treated plants. *Prismatolaimus* is relatively more abundant in the rhizosphere of BABA-treated plants, whereas it is relatively less abundant in rhizospheres of BTH or PA-treated plants. The enrichment of *Mononchus* persists at this time point in rhizospheres of plants treated with BABA, BTH or PA, but the enrichment of other minor genera does not. Also notable is a substantial enrichment in the genus *Thonus* in rhizospheres of plants treated with IR stimuli at this time point.

Changes in root nematode communities are less substantial and less consistent across treatments. At 3 dat, all three treatments lead to a root nematode community enriched in free-living, likely fungivorous, *Aphelenchoides* species and several other genera of free-living fungivorous or bacterivorous (Yeates *et al.*, 1993) nematodes. At the second time point, 14 days after treatment (dat), the only significant change is an enrichment in *Prismatolaimus*. Since none of the aforementioned nematodes are known to be endoparasitic (Yeates *et al.*, 1993) and roots were

washed thoroughly with distilled water prior to collection, these nematodes are likely tightly associated with the root surface.

Discussion

Integrated pest management (IPM) has been defined as a 'decision support system for the selection and use of pest control tactics, singly or harmoniously coordinated into a management strategy, based on cost/benefit analyses that take into account the interests of and impacts on producers, society, and the environment' (Kogan, 1998). One of the objectives of IPM programs is to preserve soil biodiversity, both for its own sake and because of its importance to plant growth and disease resistance (Rasmann and Turlings, 2016). Given the association between intensive pesticide use and diminished or altered soil biodiversity, IPM programs try to reduce pesticide usage in favor of alternatives (Thiele-Bruhn *et al.*, 2012; Jacobsen and Hjelmso, 2014; Gunstone *et al.*, 2021). This has led to increasing interest in IR stimuli as tools for managing soil pests and pathogens (Gozzo and Faoro, 2013; Desmedt *et al.*, 2021b).

However, the mechanisms of action of IR stimuli in root tissues are only partially understood, and little is known about their effect on plant-rhizosphere interactions and the root exudates which shape them. This stands in contrast to aerial plant parts, where IR stimuli are known to enhance the recruitment of beneficial arthropods by altering volatile organic compound emission from leaves (Desmedt *et al.*, 2021b). In this study, we investigate the direct effect (i.e., the effect of IR stimuli that occurs even in the absence of pest or pathogen challenge) of four chemically distinct chemical IR stimuli effective against rice root-knot nematode disease on the root transcriptome and exudome, and on rhizosphere nematode communities.

At the transcriptional level, we identified a set of genes and pathways whose expression was significantly affected by all four tested IR stimuli (see **Table 1** and **Supplementary Tables S1-S3**), as well as a significant number of shared alterations to the exudome composition (**Table 2**). Moreover, IR stimuli led to a significant but generally transient change in the structure of rhizosphere community structure, and an increased relative abundance of the predatory nematode genus *Mononchus* that persisted until at least 14 days after treatment (dat).

Differential expression analysis of our mRNA-seq data reveals two pathways that are clearly systemically induced by the four IR stimuli tested: phenylpropanoid pathway (PPP) and jasmonic acid (JA) metabolism. Interestingly, weighted gene co-expression network analysis (WGCNA) places these two pathways together in a single module (M3) that is strongly negatively correlated with the mock-treated control group. This confirms the results of the differential expression analysis, and indicates that both pathways are co-regulated during IR establishment.

Several studies have reported induction or reprogramming of PPP metabolism in response to treatment with IR stimuli in various – mainly dicot – plant species (Tugizimana *et al.*, 2018; Luna *et al.*, 2020; Gao *et al.*, 2020; Ameye *et al.*, 2020; Desmedt *et al.*, 2021a; Gamir *et al.*, 2021), which we have now confirmed at the transcriptional level in rice in response to four distinct IR stimuli. The PPP contributes directly to plant immunity through cell wall reinforcement and the production of antimicrobial secondary metabolites (Naoumkina *et al.*, 2010; Desmedt *et al.*, 2020), and evidence is also mounting for the role of various PPP derivatives as regulatory and signaling molecules in plant immunity (Desmedt *et al.*, 2021a; Huang *et al.*, 2021).

Looking at individual genes within this pathway, the induction of two *PHENYLALANINE AMMONIA-LYASE* (*PAL*) genes, *OsPAL3* and *OsPAL4*, is notable. *OsPAL4* in particular is as a key player in rice immunity against foliar diseases (Tonnessen *et al.*, 2014), and *OsPAL4* knock-out mutants are impaired in IR induction by chito-oligosaccharides and oligogalacturonides against *M. graminicola* (Singh *et al.*, 2019). Further downstream, the flavonoid biosynthesis genes *CHALCONE ISOMERASE 2* (*OsCHI2*) and *FLAVANONE-3-HYDROXYLASE* (*OsF3H*) are also induced; overexpression of either gene enhances flavonoid accumulation (Jan *et al.*, 2021; Jayaraman *et al.*, 2021), and *OsF3H* overexpression enhances resistance to bacterial blight disease (Jan *et al.*, 2021). Several genes at least tentatively associated with lignification are also induced in roots by IR stimuli. Besides the aforementioned *PAL* genes, *4-COUMARATE:COA-LIGASE 3* (*Os4CL3*) is also strongly induced by all four stimuli. *Os4CL3* knock-down causes lignin deficiency and an altered cell wall-bound phenolic compound profile (Gui *et al.*, 2011). Also worth mentioning is the strong induction of four genes encoding uclacyanin-like proteins. Their closest *A. thaliana* ortholog, according to the PLAZA integrative method (Van Bel *et al.*, 2018), is *UCLACYANIN 1*, which is involved in lignin deposition in the Casparian strip (Reyt *et al.*, 2020). Enhanced lignification upon *M. graminicola* attack in rice is associated with resistance (Galeng-Lawilao *et al.*, 2019), and primed lignification has been observed in BABA-treated rice plants upon infection by *M. graminicola* (Ji *et al.*, 2015), and in PA or BTH-treated tomato plants upon *Meloidogyne incognita* infection (Veronico *et al.*, 2018; Desmedt *et al.*, 2021a). Taken together, these results point towards a key role for altered PPP metabolism, particularly flavonoid and lignin metabolism, during IR establishment in rice roots.

The second major shared transcriptional response to IR stimuli in rice roots is the induction of JA metabolism: all tested IR stimuli induced the key JA biosynthesis genes *OsAOS1*, *OsAOC1* and *OsOPR1*. *OsJAR1*, which encodes a JASMONYL-L-ISOLEUCINE SYNTHASE enzyme that catalyzes the formation of the highly bioactive conjugate JA-isoleucine (Wasternack and Song, 2017), is also induced by all four stimuli. The importance of *OsAOC1* in rice immunity against *M. graminicola* has been functionally validated: the *OsAOC1* knock-out line *hebiba* shows increased susceptibility to *M. graminicola* (Nahar *et al.*, 2011; Riemann *et al.*, 2013).

This consistent induction of JA metabolism by chemically distinct stimuli supports that JA is the principal hormonal inducer of rice immune responses, irrespective of pathogen lifestyle (de Vleeschauwer *et al.*, 2013). By contrast, in model dicots such as *A. thaliana* salicylic acid (SA) and JA regulate largely distinct and sometimes mutually antagonistic defense responses (de Vleeschauwer *et al.*, 2013). Strikingly, BTH – an IR stimulus often described as a SA analog on account of its high affinity for the SA receptor *NPR1* (Wu *et al.*, 2012) – induces JA metabolism genes to a similar extent as the other tested IR stimuli in our study. In further support of the distinctive nature of JA signaling in rice compared to dicots, PA treatment in tomato has no effect on the expression of JA biosynthesis genes or JA content in leaves and roots (Desmedt *et al.*, 2021a). The co-regulation of JA and PPP metabolism identified by our WCGNA analysis may indicate that JA acts as a positive regulator of PPP metabolism during IR establishment, in agreement with the previously observed role of JA as a positive regulator of the biosynthesis of PPP-derived secondary metabolites in *A. thaliana* and various medicinal plant species (De Geyter *et al.*, 2012).

WCGNA also identified a module, M12, that is highly enriched in genes involved in iron homeostasis and which is positively correlated with mock-treated samples. This is consistent with literature observations associating perturbed iron homeostasis with IR and immune signaling in various plant

species and tissues, including in rice roots (Verbon *et al.*, 2017; Herlihy *et al.*, 2020; Trapet *et al.*, 2021). The clearest link between iron and IR is provided by a study showing that BABA treatment and iron deficiency show shared metabolic, transcriptional and phenotypic effects in *A. thaliana* (Koen *et al.*, 2014). Interestingly, differential expression analysis did not detect the involvement of iron homeostasis, which highlights the complementarity of gene co-expression network and differential expression analysis in transcriptome analysis.

While our results show a common transcriptional response to IR stimuli, each IR stimulus also has a unique transcriptional signature. Perhaps most obviously, the four stimuli vary greatly in the magnitude of the induced systemic transcriptional change: from 294 DE genes in BABA-treated plants to 2402 DE genes in DHA-treated plants. Despite this large difference, the four IR stimuli show a similar efficacy against *M. graminicola* in this study, which indicates that each IR stimulus induces at least some genes and pathways that are not strictly necessary for establishing an IR phenotype in young rice seedlings against *M. graminicola* at the used concentrations .

Looking at GO terms unique to each of the four stimuli (shown in **Supplementary Table S5**) reveals further differences. Both g:Profiler and PLAZA identify SA biosynthesis and signaling as affected by BTH, but not by the other compounds. This is probably caused by the high affinity of BTH for the SA receptor *NPR1*, which activates SA signaling (Wu *et al.*, 2012). Perhaps more surprisingly, this result indicates that activating SA signaling in rice in turn activates JA metabolism, in contrast both to the antagonism between both hormones that is often observed in dicot species and to the idea that SA is largely subordinate to JA in rice (de Vleeschauwer *et al.*, 2013).

For PA, g:Profiler identifies ‘cinnamic acid metabolic process’ and ‘cinnamic acid biosynthetic process’ as GO terms unique to this stimulus. This is likely explained by PA being an inhibitor of CINNAMATE-4-HYDROXYLASE, an enzyme whose substrate is *trans*-cinnamic acid (Schoch *et al.*, 2002).

DHA-treated samples are enriched in GO terms related to numerous biological processes, many of which are related to reactive oxygen species (ROS) and redox metabolism or to development. This agrees with the key regulatory role of the ascorbate/DHA balance in various developmental processes through ROS scavenging and maintenance of the redox homeostasis (Foyer *et al.*, 2020). DHA-mediated alterations to redox metabolism and ascorbate homeostasis, which are further explored in (Chavan *et al.*, 2022), may explain DHA-mediated growth inhibition in young rice seedlings.

Finally, BABA-treated samples show a unique enrichment in GO terms related to peptidase and protease activity. The *in planta* target of BABA is an aspartyl-tRNA-synthetase (Luna *et al.*, 2014) that interacts with VOZ transcription factors (Schwarzenbacher *et al.*, 2020), but to the best of our knowledge BABA-IR induction has not been associated with altered protease or peptidase activity.

After examining the shared and unique transcriptional signatures of distinct IR stimuli, we also analyzed their effect on the root exudome. As shown in **Table 2**, IR stimuli increase the exudation of amino acids such as ornithine, which might be explained by induction of JA biosynthesis upon IR treatment: in *A. thaliana*, impairment in JA signaling significantly reduces the exudation of amino acids such as ornithine (Carvalhais *et al.*, 2015). Interestingly, an *ACETYLORNITHINE TRANSAMINASE* is one of the core genes induced by IR stimuli in our data; this gene is part of the ornithine pathway from which ornithine and arginine are derived (Slocum, 2005).

Increased exudation of amino acids and fatty acids – both seen in our data – promotes recruitment of resistance-inducing *Pseudomonas* strains (Wen *et al.*, 2020), and may thus be part of a *cry for help* meant to recruit beneficial microbes (Rizaludin *et al.*, 2021). In tentative support of this hypothesis, the rhizosphere of plants treated with IR stimuli is enriched in the predatory nematode genus *Mononchus*, members of which feed on plant-parasitic nematodes (Khan and Kim, 2007). To the best of our knowledge, plant recruitment of these predatory nematodes has not been reported, but active recruitment of entomopathogenic nematodes has been observed before (Rasmann and Turlings, 2016).

In addition to attracting beneficial microbes, root exudates may also repel or antagonize attackers. Exudates from rice plants treated with IR stimuli are enriched in pelargonic acid and possibly also in hexadecanoic acid. Pelargonic acid is directly nematicidal (Chitwood, 2002), whereas hexadecenoic acid in tomato root exudates inhibits hatching and chemotaxis of the nematode *Globodera pallida* (Rizaludin *et al.*, 2021). Rice root exudates are also enriched in benzoic acid derivatives after application of IR stimuli. These metabolites are derived from the PPP, which is consistent with the transcriptional induction of phenylpropanoid metabolism. Benzoic acids exuded by rice plants may be involved in rice allelopathy (Seal *et al.*, 2004) and alter the microbial composition of rice paddy soils (Kong, 2008).

The exudome changes seen after treatment with IR stimuli are reflected by substantial but mostly transient changes in rhizosphere nematode community structure. At the earliest time point evaluated, three days after treatment (dat), IR stimuli induced a shift in the rhizosphere nematode community characterized by greater diversity, reduced abundance of *Acrobeloides* and greater abundance of *Mononchus*. By 14 dat, rhizosphere nematode communities of plants treated with BTH or PA had returned to normal, except for continued enrichment in *Mononchus*. The effect of BABA proved more persistent: rhizospheres of BABA-treated plants were impoverished in *Acrobeloides* and enriched in *Prismatolaimus*. None of the tested IR stimuli reduced rhizosphere nematode diversity (measured through Simpson's diversity index), in contrast to the negative impact of frequent nematicide use on soil biodiversity (Thiele-Bruhn *et al.*, 2012).

The reason for the reduced abundance of the bacterial-feeding genus *Acrobeloides* (Yeates *et al.*, 1993) is unclear. *A. thaliana* mutants impaired in several phytohormone signaling pathways had altered *Acrobeloides* abundance (Sikder *et al.*, 2021b), which suggests that *Acrobeloides* might be sensitive to root exudate composition. The underlying mechanism is unknown, but one possibility is that altered root exudate composition affects the composition of the bacterial communities on which *Acrobeloides* feeds. Perturbing JA metabolism or signaling significantly alters the composition of the rhizosphere bacterial community (Carvalhais *et al.*, 2013, 2015), and *Acrobeloides* species are discriminating feeders with clear preferences for certain bacterial species (Liu *et al.*, 2017). The enrichment in *Prismatolaimus*, another genus of bacterial-feeding nematodes (Yeates *et al.*, 1993), seen at the second time point in BABA-treated samples might indicate that this genus is better able to feed on the bacterial community present in the rhizosphere of BABA-treated plants, but since the feeding habits of *Prismatolaimus* are poorly understood (Yeates *et al.*, 1993) and the bacterial and fungal community composition of our samples is unknown, further experiments are needed.

The more persistent effect of BABA on rhizosphere nematode communities compared to PA and BTH is unlikely to be caused by direct toxicity towards nematodes: due to the foliar application used in

this study and precautions against run-off to soil (spraying plants in a horizontal position and watering after spraying), little BABA could have ended up in the soil. Perhaps more importantly, BABA is not acutely toxic to nematodes even at higher concentrations than those used in this study (Oka and Cohen, 2001; Oka *et al.*, 2007; Ji *et al.*, 2015). Instead, a more likely explanation is found in plant metabolism of BABA, BTH and PA. Whereas PA (Steenackers *et al.*, 2016; Desmedt *et al.*, 2021a) and BTH (Australian Pesticides and Veterinary Medicines Authority, 2007) are rapidly inactivated through conjugation to amino acids and sugars, BABA is a highly persistent compound with no known *in planta* conjugation or degradation route (Justyna and Ewa, 2013). BABA's persistence may lead to longer-lasting effects on plant exudate composition, and thus to longer-lasting effects on rhizosphere nematode communities. Further metabolomic and metagenomic analyses spanning a longer period of time after application are needed to verify this hypothesis.

Taken together, our data reveal common transcriptional responses to systemic IR in rice roots to four chemically distinct IR stimuli, which primarily involve the induction of JA biosynthesis and phenylpropanoid metabolism. IR stimuli similarly induce a set of shared perturbations to root exudate composition, characterized by increased exudation of certain amino acids, fatty acids, sugars and PPP derivatives. In turn, this leads to significant shifts in the composition of rhizosphere nematode communities. Our results thus support the existence of common responses to chemical IR stimuli with different receptors and initial signaling cascades, and highlight the interaction between IR and soil microbial communities. Such interactions may have important practical implications for the use of IR stimuli as crop protection products: if IR stimuli operate partially by promoting mutualistic plant-microbe interactions such as the recruitment of predatory nematodes, adopting soil management practices that conserve soil biodiversity (Puissant *et al.*, 2021) might enhance the efficacy of IR-based crop protection products.

Accepted Manuscript

Acknowledgements

The authors gratefully acknowledge Stefano Sacchi (Plant Health Service, Regione Lombardia, Italy) for collecting field soil for the metabarcoding experiment, and Lien De Smet and Eva Degroote (Ghent University) for technical support with mRNA extraction.

Author contribution statement

This manuscript was written by WD, with substantial input from BV, TK, MV and MN. Nematode infection experiments were performed jointly by WD and SNC. Collection of mRNA was done by WD, except for the DHA-treated plants which were grown and sampled by SNC; mRNA-seq data analysis was performed by WD. Root exudates were collected by WD, and were analyzed using GC-MS by SD. GC-MS data analysis was performed jointly by SD and WD. Metabarcoding experiments were performed jointly by WD and ENK; the resulting data was analyzed by WD, using a bioinformatics pipeline originally developed by ENK.

Conflicts of interest

WD, BV and TK are inventors of two patent applications describing the use of piperonylic acid as a crop protection product: WO2019122107A1 and WO2020127216A1. Patent WO2019122107A1 has been licensed to Eastman. The other authors have no potential conflicts of interest to disclose.

Funding

WD was financially supported a Baekeland grant (HBC.2017.0574) jointly funded by the Flemish government's Agency for Innovation and Entrepreneurship (VLAIO) and Taminco, an Eastman subsidiary. The metabarcoding experiment was performed during a stay abroad by WD in the lab of MN and MV, which was partially funded by an FWO travel grant (V415721N).

Data availability

The data that support the findings of this study are available from the corresponding author upon reasonable request. Metabarcoding sequence data has been uploaded to SRA (accession PRJNA797929), and mRNA-sequencing data to GEO (accession GSE194400).

References

- Ameye M, van Meulebroek L, Meuninck B, Vanhaecke L, Smagghe G, Haesaert G, Audenaert K.** 2020. Metabolomics Reveal Induction of ROS Production and Glycosylation Events in Wheat Upon Exposure to the Green Leaf Volatile Z-3-Hexenyl Acetate. *Frontiers in Plant Science* **11**, 1854.
- Australian Pesticides and Veterinary Medicines Authority.** 2007. *Evaluation of the new active ACIBENZOLAR-S-METHYL in the product BION PLANT ACTIVATOR SEED TREATMENT*. Canberra.
- Baetz U, Martinoia E.** 2014. Root exudates: The hidden part of plant defense. *Trends in Plant Science* **19**, 90–98.
- Van Bel M, Diels T, Vancaester E, Kreft L, Botzki A, Van De Peer Y, Coppens F, Vandepoele K.** 2018. PLAZA 4.0: An integrative resource for functional, evolutionary and comparative plant genomics. *Nucleic Acids Research* **46**, D1190–D1196.
- Bolyen E, Rideout JR, Dillon MR, et al.** 2019. Reproducible, interactive, scalable and extensible microbiome data science using QIIME 2. *Nature Biotechnology* 2019 **37**:8 **37**, 852–857.
- Byrd DW, Kirkpatrick T, Barker KR, Barker KR.** 1983. An improved technique for clearing and staining plant tissues for detection of nematodes. *Journal of nematology* **15**, 142–3.
- Carvalhais LC, Dennis PG, Badri D V., Kidd BN, Vivanco JM, Schenk PM.** 2015. Linking Jasmonic acid signaling, root exudates, and rhizosphere microbiomes. *Molecular Plant-Microbe Interactions* **28**, 1049–1058.
- Carvalhais LC, Dennis PG, Badri D V., Tyson GW, Vivanco JM, Schenk PM.** 2013. Activation of the Jasmonic Acid Plant Defence Pathway Alters the Composition of Rhizosphere Bacterial Communities. *PLOS ONE* **8**, e56457.
- Chavan SN, de Kesel J, Desmedt W, et al.** 2022. Dehydroascorbate induces plant resistance in rice against root-knot nematode *Meloidogyne graminicola*. *Molecular Plant Pathology* **00**, 1–17.
- Chitwood DJ.** 2002. Phytochemical based strategies for nematode control. *Annual Review of Phytopathology* **40**, 221–249.
- Cohen Y, Vaknin M, Mauch-Mani B.** 2016. BABA-induced resistance: milestones along a 55-year journey. *Phytoparasitica* **44**, 513–538.
- van Dam NM, Bouwmeester HJ.** 2016. Metabolomics in the Rhizosphere: Tapping into Belowground Chemical Communication. *Trends in Plant Science* **21**, 256–265.
- Desmedt W, Jonckheere W, Nguyen VH, et al.** 2021a. The phenylpropanoid pathway inhibitor piperonylic acid induces broad-spectrum pest and disease resistance in plants. *Plant, Cell & Environment* **44**, 3122–3139.

- Desmedt W, Kudjordjie EN, Chavan SN, et al.** 2022. Rice diterpenoid phytoalexins are involved in defence against parasitic nematodes and shape rhizosphere nematode communities. *New Phytologist*.
- Desmedt W, Mangelinckx S, Kyndt T, Vanholme B.** 2020. A Phytochemical Perspective on Plant Defense Against Nematodes. *Frontiers in Plant Science* **11**, 1765.
- Desmedt W, Vanholme B, Kyndt T.** 2021*b*. Plant defense priming in the field: a review. *Recent Highlights in the Discovery and Optimization of Crop Protection Products*, 87–124.
- Foyer CH, Kyndt T, Hancock RD.** 2020. Vitamin C in Plants: Novel Concepts, New Perspectives, and Outstanding Issues. *Antioxidants & Redox Signaling* **32**, 463–485.
- Galeng-Lawilao J, Kumar A, Cabasan MaTN, de Waele D.** 2019. Comparison of the penetration, development and reproduction of *Meloidogyne graminicola*, and analysis of lignin and total phenolic content in partially resistant and resistant recombinant inbred lines of *Oryza sativa*. *Tropical Plant Pathology* **44**, 171–182.
- Gamir J, Minchev Z, Berrio E, García JM, de Lorenzo G, Pozo MJ.** 2021. Roots drive oligogalacturonide-induced systemic immunity in tomato. *Plant, Cell & Environment* **44**, 275–289.
- Gao H, Zhou Q, Yang L, Zhang K, Ma Y, Xu ZQ.** 2020. Metabolomics analysis identifies metabolites associated with systemic acquired resistance in *Arabidopsis*. *PeerJ* **8**, e10047.
- De Geyter N, Gholami A, Goormachtig S, Goossens A.** 2012. Transcriptional machineries in jasmonate-elicited plant secondary metabolism. *Trends in Plant Science* **17**, 349–359.
- Ghaemi R, Pourjam E, Safaie N, Verstraeten B, Mahmoudi SB, Mehrabi R, De Meyer T, Kyndt T.** 2020. Molecular insights into the compatible and incompatible interactions between sugar beet and the beet cyst nematode. *BMC Plant Biology* **20**, 483.
- Gozzo F, Faoro F.** 2013. Systemic acquired resistance (50 years after discovery): Moving from the lab to the field. *Journal of Agricultural and Food Chemistry* **61**, 12473–12491.
- Gui J, Shen J, Li L.** 2011. Functional Characterization of Evolutionarily Divergent 4-Coumarate:Coenzyme A Ligases in Rice. *Plant Physiology* **157**, 574–586.
- Gunstone T, Cornelisse T, Klein K, Dubey A, Donley N.** 2021. Pesticides and Soil Invertebrates: A Hazard Assessment. *Frontiers in Environmental Science* **9**, 122.
- Herlihy JH, Long TA, McDowell JM.** 2020. Iron homeostasis and plant immune responses: Recent insights and translational implications. *The Journal of Biological Chemistry* **295**, 13444.
- Huang W-K, Ji H-L, Gheysen G, Kyndt T.** 2016. Thiamine-induced priming against root-knot nematode infection in rice involves lignification and hydrogen peroxide generation. *Molecular Plant Pathology* **17**, 614–624.
- Huang X, Wang Y, Lin J, Chen L, Li Y, Liu Q, Wang G, Xu F, Liu L, Hou B.** 2021. The novel pathogen-responsive glycosyltransferase UGT73C7 mediates the redirection of phenylpropanoid metabolism and promotes *SNC1* -dependent *Arabidopsis* immunity. *The Plant Journal* **107**, 149–165.

- Iwata M.** 2001. Probenazole - a plant defence activator. *Pesticide Outlook* **12**, 28–31.
- Jacobsen CS, Hjelmsø MH.** 2014. Agricultural soils, pesticides and microbial diversity. *Current Opinion in Biotechnology* **27**, 15–20.
- Jan R, Khan MA, Asaf S, Lubna, Park JR, Lee IJ, Kim KM.** 2021. Flavonone 3-hydroxylase Relieves Bacterial Leaf Blight Stress in Rice via Overaccumulation of Antioxidant Flavonoids and Induction of Defense Genes and Hormones. *International Journal of Molecular Sciences* 2021, Vol. 22, Page 6152 **22**, 6152.
- Jayaraman K, K. VR, Sevanthi AM, S.R. S, Gayatri, C. V, Mohapatra T, Mandal PK.** 2021. Stress-inducible expression of chalcone isomerase2 gene improves accumulation of flavonoids and imparts enhanced abiotic stress tolerance to rice. *Environmental and Experimental Botany* **190**, 104582.
- Ji H, Kyndt T, He W, Vanholme B, Gheysen G.** 2015. B-Aminobutyric acid-induced resistance against root-knot nematodes in rice is based on increased basal defence. *Molecular Plant Microbe Interaction* **28**, 519–533.
- Justyna PG, Ewa K.** 2013. Induction of resistance against pathogens by β -aminobutyric acid. *Acta Physiologiae Plantarum* **35**, 1735–1748.
- de Kesel J, Conrath U, Flors V, et al.** 2021. The Induced Resistance Lexicon: Do's and Don'ts. *Trends in Plant Science* **26**, 685–691.
- De Kesel J, Gómez-Rodríguez R, Bonneure E, Mangelinckx S, Kyndt T.** 2020. The Use of PTI-Marker Genes to Identify Novel Compounds that Establish Induced Resistance in Rice. *International Journal of Molecular Sciences* **21**, 317.
- Khan Z, Kim YH.** 2007. A review on the role of predatory soil nematodes in the biological control of plant parasitic nematodes. *Applied Soil Ecology* **35**, 370–379.
- Koen E, Trapet P, Brulé D, et al.** 2014. β -Aminobutyric Acid (BABA)-Induced Resistance in *Arabidopsis thaliana*: Link with Iron Homeostasis. *Molecular Plant Microbe Interaction* **27**, 1226–1240.
- Kogan M.** 1998. Integrated Pest Management: Historical Perspectives and Contemporary Developments. *Annual Review of Entomology* **43**, 243–270.
- Kong C-H.** 2008. Effects of rice allelochemicals on the microbial community of flooded paddy soil. *Allelopathy Journal* **22**, 299–309.
- Langfelder P, Horvath S.** 2008. WGCNA: An R package for weighted correlation network analysis. *BMC Bioinformatics* **9**, 1–13.
- Liu T, Yu L, Xu J, Yan X, Li H, Whalen JK, Hu F.** 2017. Bacterial traits and quality contribute to the diet choice and survival of bacterial-feeding nematodes. *Soil Biology and Biochemistry* **115**, 467–474.
- van Loon LC, Bakker PAHM, Pieterse CMJ.** 1998. Systemic resistance induced by rhizosphere bacteria. *Annual Review of Phytopathology* **36**, 453–483.

- Love MI, Huber W, Anders S.** 2014. Moderated estimation of fold change and dispersion for RNA-seq data with DESeq2. *Genome Biology* **15**, 550.
- Luna E, Flandin A, Cassan C, Prigent S, Chevanne C, Kadiri CF, Gibon Y, Pétriacq P.** 2020. Metabolomics to exploit the primed immune system of tomato fruit. *Metabolites* **10**, 96.
- Luna E, van Hulsten M, Zhang Y, et al.** 2014. Plant perception of β -aminobutyric acid is mediated by an aspartyl-tRNA synthetase. *Nature chemical biology* **10**, 450–6.
- Mantelin S, Bellafiore S, Kyndt T.** 2017. *Meloidogyne graminicola*, a major threat to rice agriculture. *Molecular Plant Pathology* **18**, 3–15.
- Mauch-Mani B, Baccelli I, Luna E, Flors V.** 2017. Defense priming: An adaptive part of induced resistance. *Annual Review of Plant Biology* **68**, 485–512.
- Mendy B, Wang'ombe MW, Radakovic ZS, Holbein J, Ilyas M, Chopra D, Holton N, Zipfel C, Grundler FMW, Siddique S.** 2017. Arabidopsis leucine-rich repeat receptor-like kinase NILR1 is required for induction of innate immunity to parasitic nematodes. *PLOS Pathogens* **13**, e1006284.
- Nahar K, Kyndt T, De Vleeschauwer D, Höfte M, Gheysen G.** 2011. The Jasmonate Pathway Is a Key Player in Systemically Induced Defense against Root Knot Nematodes in Rice. *Plant physiology* **157**, 305–316.
- Naoumkina MA, Zhao Q, Gallego-Giraldo L, Dai X, Zhao PX, Dixon RA.** 2010. Genome-wide analysis of phenylpropanoid defence pathways. *Molecular Plant Pathology* **11**, 829–846.
- Oka Y, Cohen Y.** 2001. Induced Resistance to Cyst and Root-knot Nematodes in Cereals by DL- β -amino-n-butyric Acid. *European Journal of Plant Pathology* 2001 107:2 **107**, 219–227.
- Oka Y, Cohen Y, Spiegel Y.** 2007. Local and Systemic Induced Resistance to the Root-Knot Nematode in Tomato by DL- β -Amino-n-Butyric Acid. *Phytopathology* **89**, 1138–1143.
- Oksanen J, Kindt R, Legendre P, O'Hara B, Simpson GL, Solymos P, Stevens MHH, Wagner H.** 2009. The vegan package.
- Pang Z, Chong J, Zhou G, De Lima Morais DA, Chang L, Barrette M, Gauthier C, Jacques PÉ, Li S, Xia J.** 2021. MetaboAnalyst 5.0: narrowing the gap between raw spectra and functional insights. *Nucleic Acids Research* **49**, W388–W396.
- Puissant J, Villenave C, Chauvin C, Plassard C, Blanchart E, Trap J.** 2021. Quantification of the global impact of agricultural practices on soil nematodes: A meta-analysis. *Soil Biology and Biochemistry* **161**, 108383.
- Rasmann S, Turlings TCJ.** 2016. Root signals that mediate mutualistic interactions in the rhizosphere. *Current Opinion in Plant Biology* **32**, 62–68.
- Raudvere U, Kolberg L, Kuzmin I, Arak T, Adler P, Peterson H, Vilo J.** 2019. G:Profiler: A web server for functional enrichment analysis and conversions of gene lists (2019 update). *Nucleic Acids Research* **47**, W191–W198.

- Reversat G, Boyer J, Pando-Bahuon A, Sannier C.** 1999. Use of a mixture of sand and water-absorbent synthetic polymer as substrate for the xenic culturing of plant-parasitic nematodes in the laboratory. *Nematology* **1**, 209–212.
- Reyt G, Chao Z, Flis P, Salas-González I, Castrillo G, Chao DY, Salt DE.** 2020. Uclacyanin Proteins Are Required for Lignified Nanodomain Formation within Casparian Strips. *Current Biology* **30**, 4103–4111.e6.
- Riemann M, Haga K, Shimizu T, et al.** 2013. Identification of rice Allene Oxide Cyclase mutants and the function of jasmonate for defence against *Magnaporthe oryzae*. *The Plant Journal* **74**, 226–238.
- Rizaludin MS, Stopnisek N, Raaijmakers JM, Garbeva P.** 2021. The Chemistry of Stress: Understanding the ‘Cry for Help’ of Plant Roots. *Metabolites* 2021, Vol. 11, Page 357 **11**, 357.
- Rognes T, Flouri T, Nichols B, Quince C, Mahé F.** 2016. VSEARCH: a versatile open source tool for metagenomics. *PeerJ* **4**.
- Schoch GA, Nikov GN, Alworth WL, Werck-Reichhart D.** 2002. Chemical inactivation of the cinnamate 4-hydroxylase allows for the accumulation of salicylic acid in elicited cells. *Plant physiology* **130**, 1022–31.
- Schwarzenbacher RE, Wardell G, Stassen J, Guest E, Zhang P, Luna E, Ton J.** 2020. The IBI1 Receptor of β -Aminobutyric Acid Interacts with VOZ Transcription Factors to Regulate Abscisic Acid Signaling and Callose-Associated Defense. *Molecular Plant* **13**, 1455–1469.
- Seal AN, Haig T, Pratley JE.** 2004. Evaluation of Putative Allelochemicals in Rice Root Exudates for Their Role in the Suppression of Arrowhead Root Growth. *Journal of Chemical Ecology* 2004 30:8 **30**, 1663–1678.
- Sikder MM, Vestergård M.** 2020. Impacts of Root Metabolites on Soil Nematodes. *Frontiers in Plant Science* **10**, 1792.
- Sikder MM, Vestergård M, Kyndt T, Fomsgaard IS, Kudjordjie EN, Nicolaisen M.** 2021a. Benzoxazinoids selectively affect maize root-associated nematode taxa. *Journal of experimental botany* **72**, 3835–3845.
- Sikder MM, Vestergård M, Kyndt T, Kudjordjie EN, Nicolaisen M.** 2021b. Phytohormones selectively affect plant parasitic nematodes associated with *Arabidopsis* roots. *New Phytologist* **232**, 1272–1285.
- Sikder MdM, Vestergård M, Sapkota R, Kyndt T, Nicolaisen M.** 2020. Evaluation of Metabarcoding Primers for Analysis of Soil Nematode Communities. *Diversity* 2020, Vol. 12, Page 388 **12**, 388.
- Singh RR, Chinnasri B, De Smet L, Haeck A, Demeestere K, Van Cutsem P, Van Aubel G, Gheysen G, Kyndt T.** 2019. Systemic defense activation by COS-OGA in rice against root-knot nematodes depends on stimulation of the phenylpropanoid pathway. *Plant Physiology and Biochemistry* **142**, 202–210.
- Singh RR, Verstraeten B, Siddique S, et al.** 2020. Ascorbate oxidation activates systemic defence against root-knot nematode *Meloidogyne graminicola* in rice. *Journal of Experimental Botany* **71**, 4271–4284.

Slocum RD. 2005. Genes, enzymes and regulation of arginine biosynthesis in plants. *Plant Physiology and Biochemistry* **43**, 729–745.

Steenackers WJ, Cesarino I, Klíma P, et al. 2016. The allelochemical MDCA inhibits lignification and affects auxin homeostasis. *Plant physiology* **172**, 874–888.

Thiele-Bruhn S, Bloem J, de Vries FT, Kalbitz K, Wagg C. 2012. Linking soil biodiversity and agricultural soil management. *Current Opinion in Environmental Sustainability* **4**, 523–528.

Thimm O, Bläsing O, Gibon Y, Nagel A, Meyer S, Krüger P, Selbig J, Müller LA, Rhee SY, Stitt M. 2004. MAPMAN: A user-driven tool to display genomics data sets onto diagrams of metabolic pathways and other biological processes. *Plant Journal* **37**, 914–939.

Tonnessen BW, Manosalva P, Lang JM, Baraoidan M, Bordeos A, Mauleon R, Oard J, Hulbert S, Leung H, Leach JE. 2014. Rice phenylalanine ammonia-lyase gene OsPAL4 is associated with broad spectrum disease resistance. *Plant Molecular Biology* **87**, 273–286.

Trapet PL, Verbon EH, Bosma RR, Voordendag K, Van Pelt JA, Pieterse CMJ. 2021. Mechanisms underlying iron deficiency-induced resistance against pathogens with different lifestyles. *Journal of experimental botany* **72**, 2231–2241.

Tugizimana F, Mhlongo MI, Piater LA, Dubery IA. 2018. Metabolomics in plant priming research: The way forward? *International Journal of Molecular Sciences* **19**.

Verbon EH, Trapet PL, Stringlis IA, Kruijs S, Bakker PAHM, Pieterse CMJ. 2017. Iron and Immunity. *Annual Review of Phytopathology* **55**, 355–375.

Veronico P, Paciolla C, Pomar F, De Leonardis S, García-Ulloa A, Melillo MT. 2018. Changes in lignin biosynthesis and monomer composition in response to benzothiadiazole and root-knot nematode *Meloidogyne incognita* infection in tomato. *Journal of Plant Physiology* **230**, 40–50.

De Vleeschauwer D, Djavaheri M, Bakker PAHM, Höfte M. 2008. *Pseudomonas fluorescens* WCS374r-induced systemic resistance in rice against *Magnaporthe oryzae* is based on pseudobactin-mediated priming for a salicylic acid-repressible multifaceted defense response. *Plant physiology* **148**, 1996–2012.

de Vleeschauwer D, Gheysen G, Höfte M. 2013. Hormone defense networking in rice: Tales from a different world. *Trends in Plant Science* **18**, 555–565.

Vlot AC, Sales JH, Lenk M, Bauer K, Brambilla A, Sommer A, Chen Y, Wenig M, Nayem S. 2021. Systemic propagation of immunity in plants. *New Phytologist* **229**, 1234–1250.

Wasternack C, Song S. 2017. Jasmonates: biosynthesis, metabolism, and signaling by proteins activating and repressing transcription. *Journal of Experimental Botany* **68**, 1303–1321.

Van Wees SC, Van der Ent S, Pieterse CM. 2008. Plant immune responses triggered by beneficial microbes. *Current Opinion in Plant Biology* **11**, 443–448.

Wen T, Zhao M, Yuan J, Kowalchuk GA, Shen Q. 2020. Root exudates mediate plant defense against foliar pathogens by recruiting beneficial microbes. *Soil Ecology Letters* 2020 3:1 **3**, 42–51.

Wu Y, Zhang D, Chu JY, Boyle P, Wang Y, Brindle ID, De Luca V, Després C. 2012. The Arabidopsis NPR1 Protein Is a Receptor for the Plant Defense Hormone Salicylic Acid. *Cell Reports* **1**, 639–647.

Yeates GW, Bongers T, De Goede RGM, Freckman DW, Georgieva SS. 1993. Feeding Habits in Soil Nematode Families and Genera - An Outline for Soil Ecologists. *Journal of Nematology* **25**, 315–331.

Zhang Y, Parmigiani G, Johnson WE. 2020. ComBat-seq: batch effect adjustment for RNA-seq count data. *NAR Genomics and Bioinformatics* **2**.

Accepted Manuscript

Figure legends

Figure 1: Effect of different chemical IR stimuli on rice resistance to *M. graminicola*. **(a)** Number of galls per root system present 14 days after inoculation with 250 *M. graminicola* J2s. **(b)** Shoot length of plants harvested 14 days after inoculation. **(c)** Root length of plants harvested 14 days after inoculation. Treatments with different letters are significantly different ($p < 0.05$), according to the non-parametric Conover-Iman post-hoc test. $N = 8$. Abbreviations: BABA – 3.5 mM β -aminobutyric acid, applied foliarly one day before inoculation; BTH - 250 μ M acibenzolar-S-methyl, applied foliarly one day before inoculation; DHA – 20 mM dehydroascorbic acid, applied one day before inoculation; PA 1x – 300 μ M piperonylic acid, applied foliarly one day before inoculation; PA 2x – 300 μ M piperonylic acid, applied foliarly one and seven days before inoculation. Cross indicate means, horizontal bars indicate medians. The bottom and top of each box indicate the 25th and 75th percentile, and the whiskers the 25th percentile – 1.5 times the interquartile range and the 75th percentile + 1.5 times the interquartile range respectively.

Figure 2: Exploratory analysis of the effect of distinct IR stimuli on rice roots. **(a)** PCA scores plot showing the separation of the transcriptomes of mock-, BABA-, BTH- and PA-treated roots along the first and second principal component axes. Since DHA-data are derived from a separate experiment, it is not shown in this figure. **(b)** Venn diagram showing the number of differentially expressed genes (relative to mock-treated plants) for each treatment.

Figure 3: **(a)** PCA scores plot showing the exudomes of plants treated with the IR stimuli PA, BABA and BTH, and/or with the nematode PAMP solution NemaWater (NW). **(b-c)** PCA scores plot showing the exudomes of plants treated with the IR stimuli PA, BABA and BTH (b) or with NW (c). **(d)** Venn diagram showing differentially abundant features between plants treated with BABA, BTH, PA or NW and mock-treated plants. **out** Venn diagram showing ‘primed’ features, i.e. features whose abundance differs between mock-treated, NW-induced plants and BABA, BT or PA-treated plants induced with NW.

Figure 4: Non-metric multi-dimensional scaling (NMDS) of nematode communities in the rhizosphere and root system of rice plants treated with the IR stimuli BABA, BTH or PA, or with a mock treatment. **(a)** Rhizosphere, 3 days after treatment (dat). **(b)** Root system, 3 dat. **(c)** Rhizosphere, 14 dat. **(d)** Root system, 14 dat. NMDS stress values: (a) 0.11; (b) 0.11; (c) 0.13; (d) 0.17.

Figure 5: Relative abundance of detected nematode taxonomic units in rhizosphere soil sampled three days after treatment (17 days post transplantation) **(a)**, in roots sampled three days after treatment **(b)**, in rhizosphere soil sampled 14 days after treatment **(c)** and in roots sampled 14 days after treatment **(d)** in mock-treated plants or in plants treated with the IR stimuli BABA, BTH and PA. ‘Other’ consists of minor genera representing less than 1% of reads in a sample; ‘Unknown’ refers to nematode OTUs that could not be assigned to genus level. Note: Dorylaimoidea is a superfamily rather than genus; this group contains a highly abundant OTU with > 99% sequence similarity to accessions belonging to multiple genera in this superfamily and could thus not be assigned to genus level. Taxons whose relative abundance differs significantly between genotypes are shown with an ‘*’ in the figure legend (Kruskal-Wallis, $p < 0.10$). Groups that differ significantly from the mock-treated control according to the Conover-Iman post-hoc test are indicated with asterisks in the bar chart itself (*: $p < 0.10$; **: $p < 0.01$, ***: $p < 0.001$). $N = 5$.

Table 1: List of genes that are significantly differentially expressed (FDR-adjusted $P < 0.10$) in rice roots 24 h after treatment with either BABA, BTH, DHA or PA. Values in the table indicate the \log_2 -fold change relative to mock-treated samples. Gene names were obtained using the RAPDB database (with manual curation), and were manually assigned to categories based on gene function.

Locus	Name	Category	BABA	BTH	DHA	PA
Os03g0236200	Glutamate decarboxylase 3	GABA biosynthesis	0.8	0.8	0.8	0.7
Os07g0154100	9- <i>cis</i> -Epoxy-carotenoid dioxygenase NCED4	Hormone, ABA biosynthesis	0.8	0.9	1.2	0.6
Os03g0438100	Allene oxide cyclase (OsAOC1)	Hormone, JA biosynthesis	0.5	0.6	0.9	0.5
Os03g0767000	Allene oxide synthase (OsAOS1)	Hormone, JA biosynthesis	0.5	0.7	1.5	0.8
Os05g0586200	Jasmonyl-L-isoleucine synthase 1 (OsJAR1)	Hormone, JA biosynthesis	0.6	0.9	0.9	0.7
Os06g0216300	12-Oxo-phytodienoic acid reductase 1 (OsOPR1)	Hormone, JA biosynthesis	0.7	1.3	2.1	0.6
Os07g0461900	Acetylornithine transaminase	Metabolism, amino acid (arginine)	0.5	1.1	0.8	0.6
Os03g0290300	Fatty acid desaturase 7	Metabolism, fatty acids	0.7	0.8	2.5	0.7
Os02g0525600	Acetyl-coenzyme A synthetase	Metabolism, general	-0.6	-0.8	-0.5	-0.7
Os01g0628700	Cytochrome P450 CYP72A24	Metabolism, general	0.6	0.7	0.8	0.8
Os04g0497000	NADPH oxidoreductase 1	Metabolism, general	0.8	0.9	1.0	0.7
Os07g0418500	Cytochrome P450 CYP709C9	Metabolism, general	1.4	2.3	1.8	2.8
Os07g0635500	Cytochrome P450 CYP709C5	Metabolism, general	0.6	0.8	1.0	0.6
Os12g0150200	Cytochrome P450 CYP94C2b	Metabolism, general	0.7	1.1	1.4	1.2
Os12g0582700	Cytochrome P450 CYP81P1	Metabolism, general	0.8	1.2	0.7	0.6
Os02g0626600	Phenylalanine ammonia-lyase 3 (OsPAL3)	PPP (central)	0.6	1.0	1.6	0.8
Os02g0627100	Phenylalanine ammonia-lyase 4 (OsPAL4)	PPP (central)	0.6	1.0	2.2	0.7
Os03g0122300	Flavanone 3-hydroxylase	PPP (flavonoids)	0.8	1.7	0.9	0.8
Os06g0203600	Chalcone isomerase 2 (OsCHI2)	PPP (flavonoids)	0.5	0.6	1.0	0.6

Os07g0526400	Polyketide synthase 15 / Chalcone synthase 15	PPP (flavonoids)	1.5	2.3	2.8	1.5
Os09g0543900	Putrescine hydroxycinnamoyltransferase 3	PPP (HCAA)	0.6	0.9	2.1	0.8
Os02g0177600	4-Coumarate:coenzyme A ligase 3	PPP (lignification)	0.6	0.9	1.1	0.7
Os08g0137800	Uclacyanin-like protein 24	PPP (lignification)	1.0	1.2	2.4	1.4
Os08g0137900	Uclacyanin-like protein 25	PPP (lignification)	0.8	0.8	2.8	1.0
Os08g0138100	Uclacyanin-like protein 26	PPP (lignification)	0.9	0.8	1.3	1.1
Os08g0138200	Uclacyanin-like protein 27	PPP (lignification)	1.0	1.0	1.5	1.1
Os05g0515600	<i>O</i> -Methyltransferase ZRP4	PPP (suberin)	1.2	0.9	1.8	1.4
Os01g0132000	Wound-induced protease inhibitor WIP1	PR	0.9	0.8	0.9	1.2
Os02g0605900	Chitinase 6, PR3	PR	1.1	1.3	0.8	1.0
Os10g0542900	Chitinase 8, PR3	PR	0.7	0.6	1.0	0.7
Os05g0495900	β -1,3-glucanase 8 (OsGns8)	PR (putative)	0.7	0.8	1.2	0.7
Os10g0147200	Thaumatococcus-like protein	PR (putative)	0.6	0.8	1.5	0.8
Os07g0162400	Cell death associated protein 1 (OsCDAP1)	Programmed cell death	0.7	1.2	1.2	1.3
Os04g0600300	Alternative oxidase 1b (OsAOX1b)	Redox metabolism	1.0	1.0	1.0	1.5
Os08g0189400	Germin-like protein 8-5	Redox metabolism	1.1	1.5	1.0	1.4
Os12g0154700	Germin-like protein 12-1	Redox metabolism	1.2	1.6	1.0	1.3
Os12g0154800	Germin-like protein 12-2	Redox metabolism	1.0	1.4	0.5	1.5
Os03g0230300	Browning of callus 1 (BOC1)	Redox metabolism	0.7	1.0	1.0	0.7
Os09g0367700	Tau class glutathione S-transferase 5	Redox metabolism	0.8	1.9	2.4	1.6
Os02g0466400	Inositol 1,3,4-trisphosphate 5/6-kinase 4	Signaling, calcium	0.6	0.9	1.7	0.9
Os03g0203700	Ca ²⁺ -ATPase 1	Signaling, calcium	0.5	0.9	1.4	0.6

Os02g0224100	Protein phosphatase 2C12	Signaling, general	-0.7	-1.1	-0.6	-0.8
Os01g0806200	F-box protein 45	Signaling, general	0.6	0.8	1.6	0.8
Os02g0548700	Plant U-box-containing protein 43	Signaling, general	0.6	0.8	1.1	0.7
Os03g0240600	U-box containing E3 ligase	Signaling, general	0.7	0.9	1.8	1.4
Os05g0588900	AAA-ATPase1	Signaling, general	0.8	0.8	1.2	0.9
Os07g0192000	AAA-ATPase	Signaling, general	0.6	0.6	0.5	0.7
Os12g0147800	Phytosulfokine 3 (OsPSK3)	Signaling, growth	0.6	1.0	0.5	0.5
Os03g0667100	NPR1 paralog 3 (OsNPR3)	Signaling, immunity	0.6	0.9	0.5	0.7
Os03g0407900	Receptor-like cytoplasmic Kinase 110	Signaling, RLK	0.5	0.9	1.8	0.8
Os07g0550900	S-Domain receptor like kinase-40	Signaling, RLK	0.8	1.1	1.7	0.9
Os02g0270200	Subtilisin 14	Signaling, stress	1.1	1.5	0.8	1.5
Os05g0474800	WRKY70	Transcription factor	0.6	0.7	0.7	0.9
Os02g0181300	WRKY71	Transcription factor	0.5	0.6	0.8	0.6
Os01g0821300	WRKY108	Transcription factor	0.6	1.2	1.5	0.6
Os01g0773800	Basic helix-loop-helix protein 185	Transcription factor	1.0	1.1	2.5	0.9
Os01g0839100	Zinc finger protein 179	Transcription factor	0.7	0.8	1.0	0.8
Os01g0862800	NAC domain-containing protein ENAC1	Transcription factor	0.8	1.0	1.0	0.6
Os02g0539200	Zinc finger RING/FYVE/PHD-type domain protein	Transcription factor	0.8	0.8	1.7	0.7
Os02g0764700	Ethylene response factor 103	Transcription factor	1.0	0.9	0.8	0.6
Os05g0132700	MYB transcription factor domain containing protein	Transcription factor	0.8	1.1	1.8	1.1
Os05g0444200	DLN repressor 142	Transcriptional regulator	0.5	1.4	2.5	0.6
Os01g0609900	ABC transporter ABCG37	Transport	0.5	0.9	1.5	0.7

Os01g0723800	MDR-like ABC transporter MDR17	Transport	0.5	0.8	0.6	0.6
Os07g0561800	Carbohydrate transporter / sugar porter	Transport	0.9	1.1	0.7	0.9
Os01g0305200	Lg106-like family protein	Unknown	0.6	0.8	0.7	0.6
Os01g0952900	Hypothetical protein	Unknown	0.9	1.1	1.1	1.1
Os03g0252100	Alpha/beta hydrolase fold-3 domain containing protein	Unknown	0.8	1.2	1.1	0.9
Os03g0318400	Peptidase A1 domain containing protein	Unknown	0.7	1.2	1.6	0.7
Os03g0797300	Similar to benzoxazinless 1	Unknown	1.1	1.5	2.5	1.0
Os04g0585000	Similar to RING-H2 finger protein ATL1R	Unknown	1.0	1.3	0.9	1.0
Os04g0639000	Hypothetical protein	Unknown	0.6	0.9	1.6	0.9
Os05g0465000	Hypothetical protein	Unknown	0.7	1.6	1.0	0.9
Os08g0364900	Similar to Pirin-like protein	Unknown	0.7	1.3	2.2	0.5
Os02g0586000	Hypothetical protein	Unknown	1.6	1.0	1.5	1.2
Os11g0618300	Hypothetical protein	Unknown	1.1	1.5	0.6	1.0

Table 2: Features annotated with a high degree of confidence (NIST match factor > 70) that are differentially abundant in exudates from rice roots collected four days after treatment with BABA, BTH, PA or NemaWater, with their retention times and log₂-fold change relative to exudates from mock-treated plants. Significant differences (FDR-adjusted p < 0.10) are highlighted in bold; cells showing increased abundance are shaded in blue, those showing reduced abundance in red. 'NQ' (non-quantifiable) indicates that a peak was either not detected or not quantifiable in a certain treatment group.

RT (min)	Annotation	Category	BABA	BTH	PA	NemaWater
22.75	Glycerol-3-phosphate	Alcohol	2.3	1.5	2.9	3.3
16.98	Triethylene glycol	Alcohol	3.1	2.0	4.2	1.9
32.62	Triethylene glycol	Alcohol	2.2	0.8	4.3	2.1
16.33	2-Nonanol	Alcohol, volatile	1.2	0.8	1.4	1.2
12.98	Pinacolyl alcohol	Alcohol, volatile	1.8	0.6	1.1	2.3
10.61	<i>N</i> -Allyloxycarbonyl- <i>d</i> -proline allyl ester	Amino acid	2.4	1.7	-1.0	3.1
11.81	Isoleucine	Amino acid	0.8	0.6	1.4	1.0
12.71	<i>N</i> -Methyl- <i>N</i> -(but-3-yn-1-yloxycarbonyl)- <i>L</i> -leucine hexadecyl ester	Amino acid	0.6	0.0	0.9	1.1
13.44	Serine	Amino acid	1.2	0.8	1.6	1.2
14.06	Threonine	Amino acid	1.3	0.9	1.7	1.6
17.43	Pyroglutamic acid	Amino acid	1.0	0.7	0.7	1.0
19.56	Ornithine	Amino acid	2.0	2.0	1.5	1.6
19.83	Phenylalanine	Amino acid	0.7	0.4	0.6	0.5
13.56	Pelargonic acid	Fatty acid	1.3	0.1	1.1	1.8
34.90	Oleamide	Fatty acid derivative	-4.9	-1.0	-6.9	-6.0
18.05	3-Methylsalicylic acid	Phenylpropanoid (benzoic acids)	2.2	1.0	2.3	2.9
24.02	Protocatechoic acid	Phenylpropanoid (benzoic acids)	2.6	2.3	NQ	2.1
15.99	3,4-Dihydroxybenzaldehyde	Phenylpropanoid (derived)	1.3	1.7	2.5	2.0
23.75	D-(-)-Fructofuranose	Sugar	2.1	0.2	1.8	1.5

23.91	D-(+)-Talofuranose	Sugar	2.2	2.6	2.6	2.0
38.03	Sucrose	Sugar	1.5	0.5	1.5	1.2
29.14	Scyllo-inositol	Sugar alcohol	3.2	2.0	3.8	3.6
10.27	3,5-Dimethylphenol	Other	0.9	0.8	1.0	1.8
10.70	Dimethoxymethyl-hydroxy-triphenyl phosphide	Other	0.5	0.2	0.6	0.8
10.94	N-(2-Hydroxyethyl)-N-methyl-perfluorobutane-1-sulfonamide	Other	-3.2	-0.2	-3.2	-3.2
11.21	1-Hydroxycyclohexanecarboxylic acid	Other	1.3	1.2	1.0	0.8
14.58	(R)-5-Methylhydantoin	Other	2.7	0.8	2.2	1.9
15.78	Methyl-2-methyl-2-methoxy-3-hydroxyindan-1-one-3-carboxylate	Other	1.4	0.9	1.7	2.2
17.16	1-(4-Methoxyphenyl)propane-1,2-diol	Other	2.3	2.2	2.4	2.5
21.07	2,5-Di-tert-butyl-4-((trimethylsilyl)oxy)phenol	Other	2.8	2.1	1.9	2.2
22.63	2-Benzyl-4-methylphenol	Other	-2.9	-1.7	-2.9	-2.9
22.90	N-(3-nitrophenyl)-3-methoxybenzamide	Other	0.6	0.6	0.7	0.8
29.28	9-(Z)-Octadecenitrile	Other	-3.4	-0.5	-4.8	-5.2
14.36	3-Butyl-3-methyl-1-hydroxycyclohexene	Other	0.7	0.4	0.6	1.0
19.04	1H-Pyrazole	Other	1.8	0.7	2.6	3.1

Table 3: permutational analysis of variance (PERMANOVA) of nematode communities in plants treated with IR stimuli compared to mock-treated plants at three and 14 days after treatment (dat).

Compartment	Time point	Comparison	R ²	P-value
Rhizosphere	3 dat	Overall	0.35	0.002
		Mock vs. BABA	0.48	0.030
		Mock vs. BTH	0.32	0.028
		Mock vs. PA	0.23	0.061
Root	3 dat	Overall	0.57	< 0.001
		Mock vs. BABA	0.08	0.441
		Mock vs. BTH	0.58	0.009
		Mock vs. PA	0.45	0.005
Rhizosphere	14 dat	Overall	0.53	< 0.001
		Mock vs. BABA	0.60	0.014
		Mock vs. BTH	0.16	0.159
		Mock vs. PA	0.08	0.597
Root	14 dat	Overall	0.15	0.534
		Mock vs. BABA	0.06	0.760
		Mock vs. BTH	0.10	0.491
		Mock vs. PA	0.12	0.363

Table 4: Differences in the abundance of identified taxonomic units between genotypes. All values shown are log₂-fold changes relative to mock-treated plants at the same time point. Asterisks indicate statistical significance, as indicated using DeSeq2 (*: FDR-adjusted p < 0.05; **: FDR-adjusted p < 0.01; ***: FDR-adjusted p < 0.001). ‘Other’ is the sum of all OTUs of nematode origin but which could not be assigned to genus or family level. Cells showing increased abundance are shaded in blue, those showing reduced abundance in red.

Taxon	3 days after treatment						14 days after treatment					
	Rhizosphere			Root			Rhizosphere			Root		
	BABA	BTH	PA	BABA	BTH	PA	BABA	BTH	PA	BABA	BTH	PA
<i>Achromadora</i>	-3.5 *	-3.9 *	2.3	ND	ND	ND	ND	ND	ND	ND	ND	ND
<i>Acrobeloides</i>	-1.5 **	-1.6 ***	-1.2 **	-0.2	0.4	0.5	-0.9 *	-0.3	-0.6 *	-0.1	-0.4	0.5
<i>Aphelenchoides</i>	0.0	4.4	2.9	4.8 **	5.4 ***	7.1 ***	-3.4 *	-1.8	0.5	-0.3	-1.6	-1.0
<i>Aporcellaimus</i>	ND	0.4	-1.1	ND	ND	ND	1.9	1.6	-0.7	ND	ND	ND
<i>Diploscapter</i>	-2.1	-1.4	-0.7	1.7	2.3 *	5.0 ***	-2.6	0.9	-1.8	-5.6 **	-0.1	-3.1
<i>Ditylenchus</i>	-6.0 ***	-2.4	-6.5 ***	5.0 *	5.8 ***	0.0	0.1	-2.3	-3.2	0.0	0.0	5.5
Dorylaimoidea	-0.9 *	0.1	-1.4 **	0.7	-2.0 **	-3.6 ***	0.1	-1.3	-0.4	1.8	0.6	2.6 *
<i>Filenchus</i>	-1.3 *	-0.8	-0.2	-0.1	-0.3	0.6	-0.0	0.9 *	0.6	-0.5	-0.2	-0.3
<i>Meloidogyne</i>	2.7 **	3.8 ***	0.2	1.3	1.8 *	-1.0	0.9	-0.3	-0.4	-0.1	0.5	-0.1
<i>Mononchus</i>	2.5 **	3.1 ***	3.2 ***	ND	ND	ND	2.5 *	3.1 **	2.6 *	ND	ND	ND
<i>Plectus</i>	-7.1 **	-1.3	-7.6 ***	3.4 *	-3.0	5.3 ***	ND	ND	ND	ND	ND	ND
<i>Pratylenchus</i>	ND	ND	ND	-3.2	-4.2	-3.8	ND	ND	ND	ND	ND	ND
<i>Prismatolaimus</i>	-1.6 **	-2.0 ***	0.3	-0.7	-5.2 **	-0.5	1.0 *	-1.6 **	-1.7 **	6.0 ***	4.5 *	4.4 *
<i>Rhabditis</i>	1.0	-1.4	1.2	ND	ND	ND	-2.0	-0.3	-1.5	ND	ND	ND
<i>Rhabdolaimus</i>	1.2 *	-0.1	0.0	3.6	2.7	1.0	1.6	2.7 *	2.9 *	-0.8	-0.4	3.1
<i>Thonus</i>	0.0	8.4 **	0.0	ND	ND	ND	7.6 ***	9.6 ***	5.7 ***	ND	ND	ND
Other	1.5 **	0.8	1.4 *	-0.2	0.1	0.2	-0.0	1.4 *	0.6	-0.8	0.2	-0.7

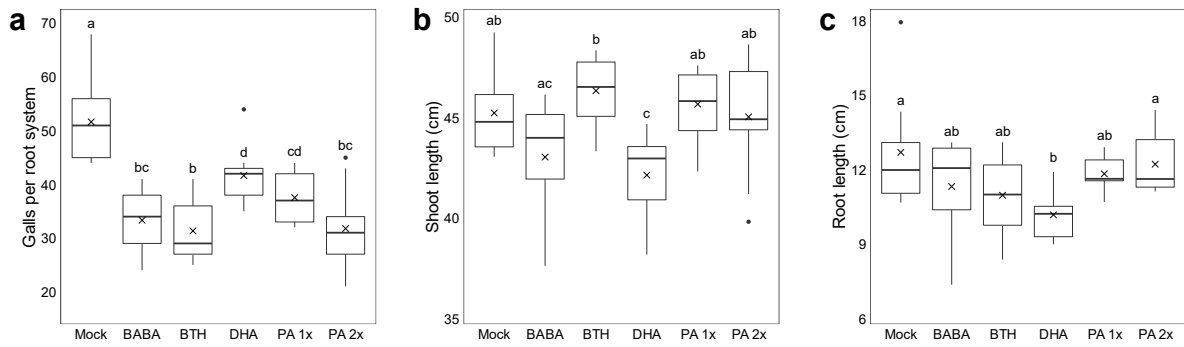


Figure 1: Effect of different chemical IR stimuli on rice resistance to *M. graminicola*. **(a)** Number of galls per root system present 14 days after inoculation with 250 *M. graminicola* J2s. **(b)** Shoot length of plants harvested 14 days after inoculation. **(c)** Root length of plants harvested 14 days after inoculation. Treatments with different letters are significantly different ($p < 0.05$), according to the non-parametric Conover-Iman post-hoc test. $N = 8$. Abbreviations: BABA – 3.5 mM β -aminobutyric acid, applied foliarly one day before inoculation; BTH - 250 μ M acibenzolar-S-methyl, applied foliarly one day before inoculation; DHA – 20 mM dehydroascorbic acid, applied one day before inoculation; PA 1x – 300 μ M piperonylic acid, applied foliarly one and seven days before inoculation. Cross indicate means, horizontal bars indicate medians. The bottom and top of each box indicate the 25th and 75th percentile, and the whiskers the 25th percentile – 1.5 times the interquartile range and the 75th percentile + 1.5 times the interquartile range respectively.

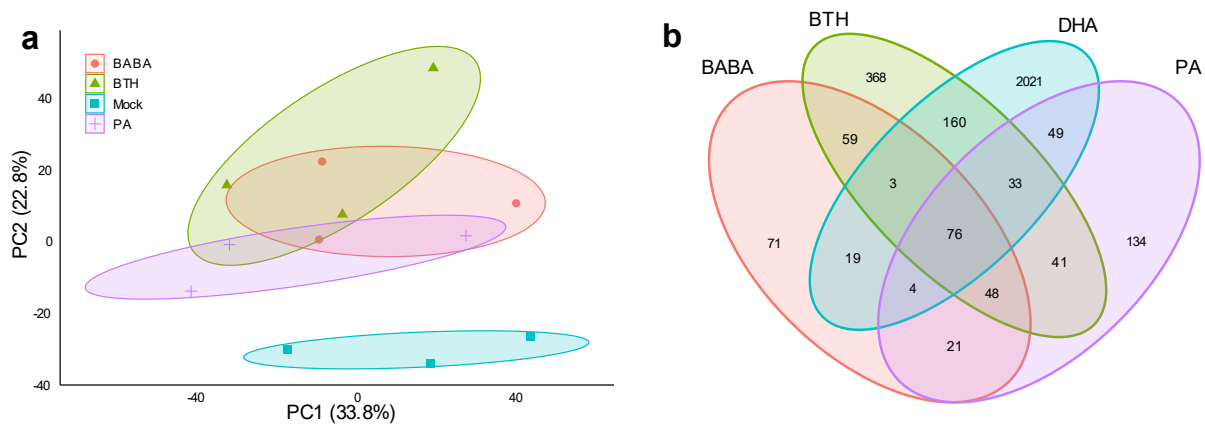


Figure 2: Exploratory analysis of the effect of distinct IR stimuli on rice roots. **(a)** PCA scores plot showing the separation of the transcriptomes of mock-, BABA-, BTH- and PA-treated roots along the first and second principal component axes. Since DHA-data are derived from a separate experiment, it is not shown in this figure. **(b)** Venn diagram showing the number of differentially expressed genes (relative to mock-treated plants) for each treatment.

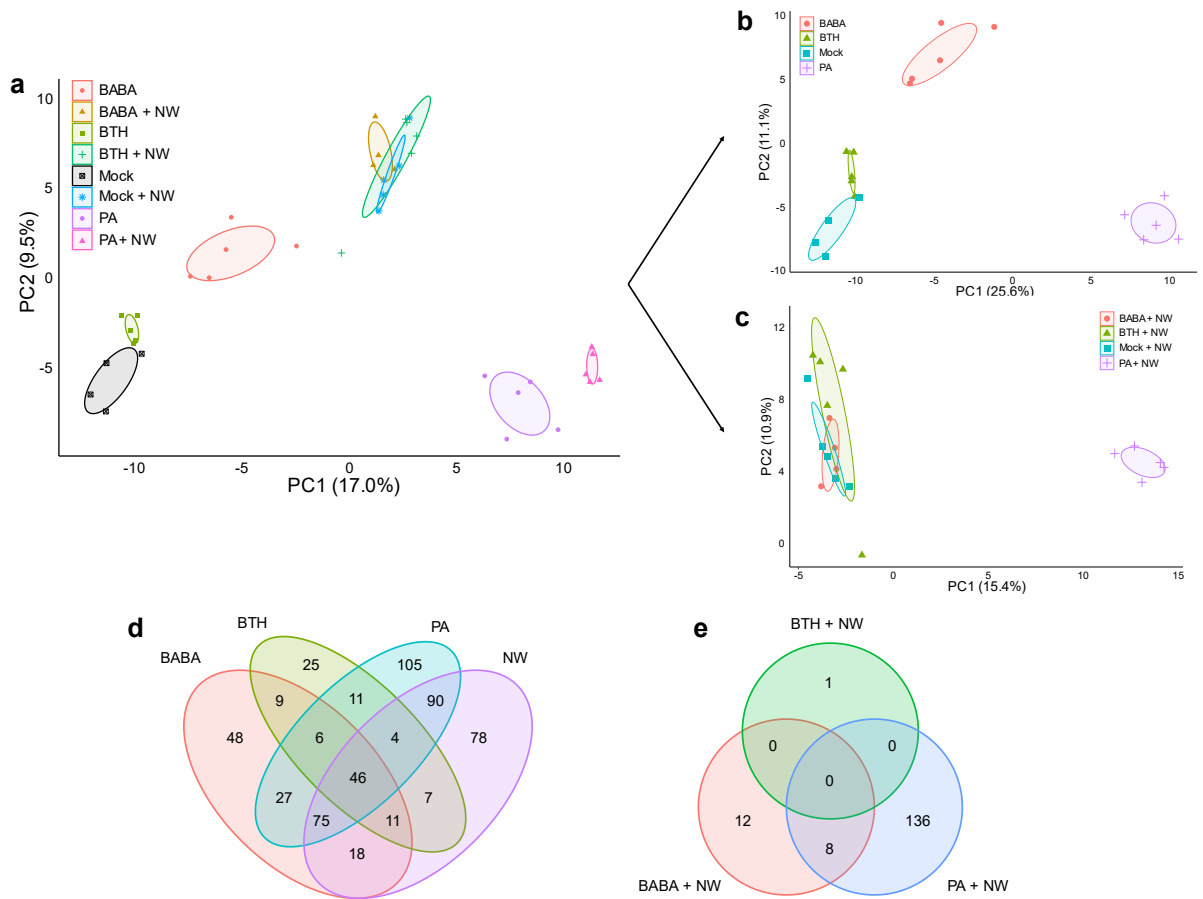


Figure 3: (a) PCA scores plot showing the exudomes of plants treated with the IR stimuli PA, BABA and BTH, and/or with the nematode PAMP solution NemaWater (NW). (b-c) PCA scores plot showing the exudomes of plants treated with the IR stimuli PA, BABA and BTH (b) or with NW (c). (d) Venn diagram showing differentially abundant features between plants treated with BABA, BTH, PA or NW and mock-treated plants. (e) Venn diagram showing 'primed' features, i.e. features whose abundance differs between mock-treated, NW-induced plants and BABA, BT or PA-treated plants induced with NW.

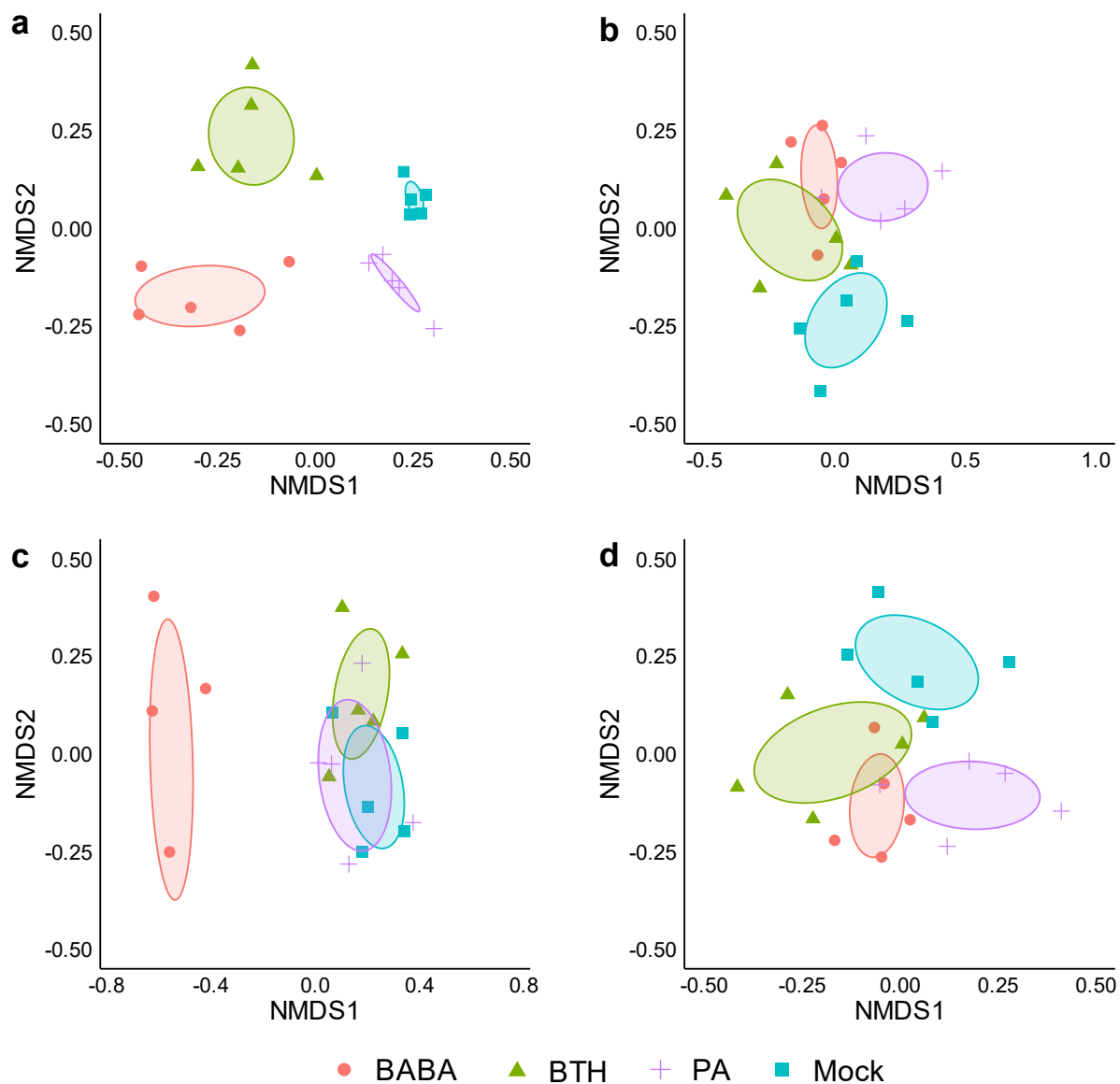


Figure 4: Non-metric multi-dimensional scaling (NMDS) of nematode communities in the rhizosphere and root system of rice plants treated with the IR stimuli BABA, BTH or PA, or with a mock treatment. **(a)** Rhizosphere, 3 days after treatment (dat). **(b)** Root system, 3 dat. **(c)** Rhizosphere, 14 dat. **(d)** Root system, 14 dat. NMDS stress values: (a) 0.11; (b) 0.11; (c) 0.13; (d) 0.17.

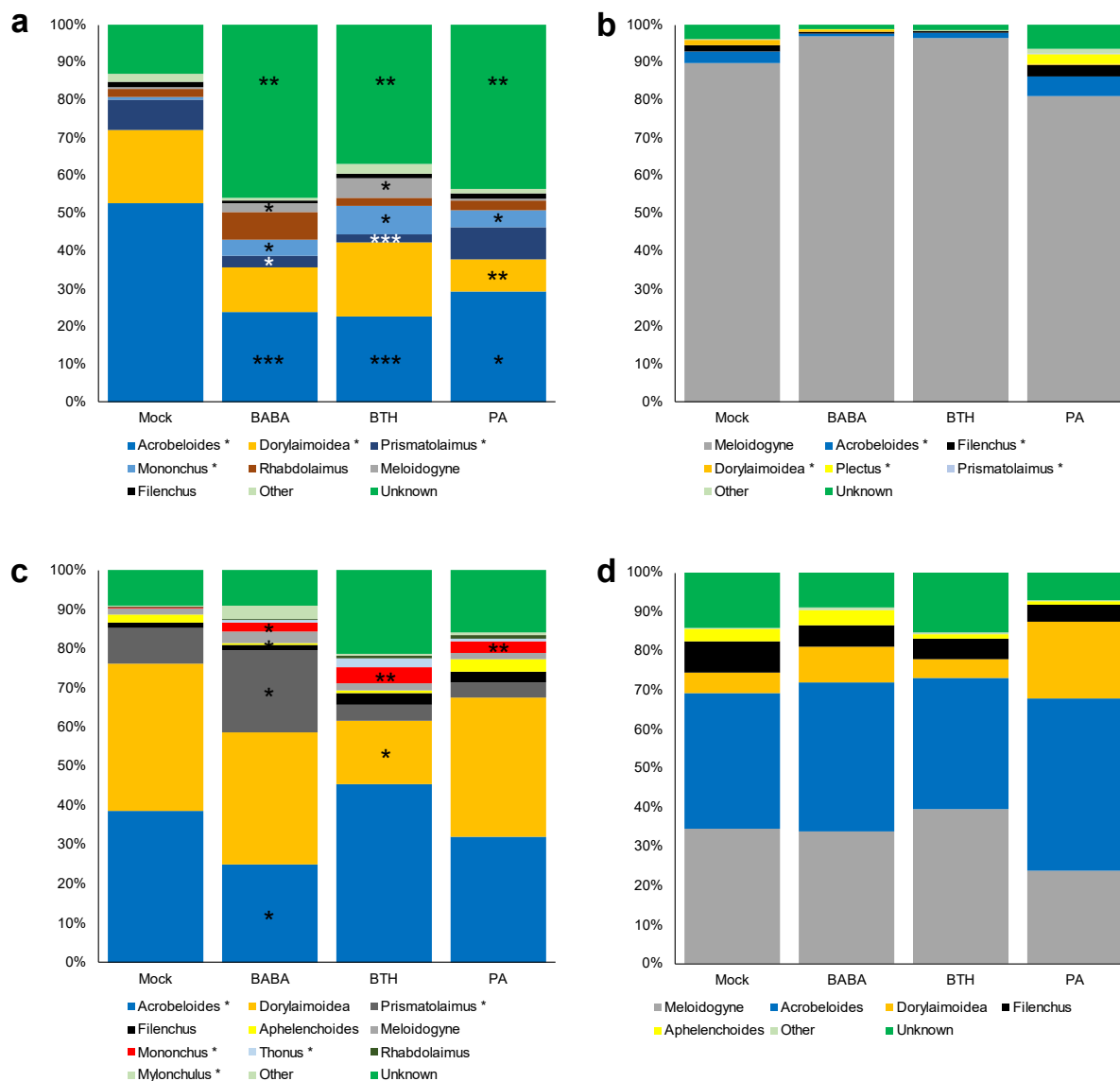


Figure 5: Relative abundance of detected nematode taxonomic units in rhizosphere soil sampled three days after treatment (17 days post transplantation) (a), in roots sampled three days after treatment (b), in rhizosphere soil sampled 14 days after treatment (c) and in roots sampled 14 days after treatment (d) in mock-treated plants or in plants treated with the IR stimuli BABA, BTH and PA. ‘Other’ consists of minor genera representing less than 1% of reads in a sample; ‘Unknown’ refers to nematode OTUs that could not be assigned to genus level. Note: Dorylaimoidea is a superfamily rather than genus; this group contains a highly abundant OTU with > 99% sequence similarity to accessions belonging to multiple genera in this superfamily and could thus not be assigned to genus level. Taxons whose relative abundance differs significantly between genotypes are shown with an ‘*’ in the figure legend (Kruskal-Wallis, $p < 0.10$). Groups that differ significantly from the mock-treated control according to the Conover-Iman post-hoc test are indicated with asterisks in the bar chart itself (*: $p < 0.10$; **: $p < 0.01$, ***: $p < 0.001$). N = 5.